

Recent Advances in the Linearized Semiclassical Initial Value Representation/Classical Wigner Model for the Thermal Correlation Function

Jian Liu

This article focuses on most recent advances in the linearized semiclassical initial value representation (LSC-IVR)/classical Wigner model that includes quantum effects with classical trajectories and recovers exact thermal correlation functions (of even nonlinear operators, that is, nonlinear functions of position or momentum operators) in the classical, high temperature, and harmonic limits. Two methods for implementing the LSC-IVR/classical Wigner which are in principle feasible to be combined with general force fields or even *ab initio* electronic

structure methods have been reviewed. One is the local Gaussian approximation with the imaginary time path integral approach, the other is the quantum thermal bath method. The article emphasizes on the theory and the algorithms for implementation, while it also covers recent applications and limitations of the LSC-IVR/classical Wigner. © 2015 Wiley Periodicals, Inc.

DOI: 10.1002/qua.24872

Introduction

There is currently a great deal of theoretical effort focused on developing ways for including quantum mechanical effects in molecular dynamics (MD) simulations,^[1–5] most of which are based on the time correlation function approach as most dynamical quantities of interest can be expressed in terms of thermal correlation functions.^[6–8] For example, velocity correlation functions can be used to calculate diffusion constants, dipole moment correlation functions are related to infrared absorption spectra, flux correlation functions yield reaction rates, energy current correlation functions produce thermal conductivities, and vibrational energy relaxation (VER) rate constants can be expressed in terms of force correlation functions. Thermal correlation functions are of the form

$$C_{AB}(t) \equiv \langle A(0)B(t) \rangle = \frac{1}{Z} \text{Tr} \left(\hat{A}^\beta e^{i\hat{H}t/\hbar} \hat{B} e^{-i\hat{H}t/\hbar} \right), \quad (1)$$

where $\hat{A}_{\text{std}}^\beta = e^{-\beta\hat{H}} \hat{A}$ for the standard version of the correlation function, or $\hat{A}_{\text{sym}}^\beta = e^{-\beta\hat{H}/2} \hat{A} e^{-\beta\hat{H}/2}$ for the symmetrized version,^[9] or $\hat{A}_{\text{Kubo}}^\beta = \frac{1}{\beta} \int_0^\beta d\lambda e^{-(\beta-\lambda)\hat{H}} \hat{A} e^{-\lambda\hat{H}}$ for the Kubo-transformed version.^[10] These three versions are related to one another by the following identities between their Fourier transforms,

$$\frac{\beta\hbar\omega}{1 - e^{-\beta\hbar\omega}} I_{AB}^{\text{Kubo}}(\omega) = I_{AB}^{\text{std}}(\omega) = e^{\beta\hbar\omega/2} I_{AB}^{\text{sym}}(\omega), \quad (2)$$

where $I_{AB}(\omega) = \int_{-\infty}^{\infty} dt e^{-i\omega t} C_{AB}(t)$ and so forth. Here, $Z = \text{Tr} [e^{-\beta\hat{H}}]$ ($\beta = 1/k_B T$) is the partition function, \hat{H} the (time-independent) Hamiltonian of the system with the total number of degrees of freedom N , which we assume to be of standard Cartesian form

$$\hat{H} = \frac{1}{2} \hat{\mathbf{p}}^T \mathbf{M}^{-1} \hat{\mathbf{p}} + V(\hat{\mathbf{x}}), \quad (3)$$

where \mathbf{M} is the diagonal 'mass matrix' with elements $\{m_j\}$, and $\hat{\mathbf{p}}$ and $\hat{\mathbf{x}}$ are the momentum and coordinate operators,

respectively; and \hat{A} and \hat{B} are operators relevant to the specific property of interest. Note that \hat{A} and \hat{B} are often *nonlinear* operators (i.e., *nonlinear* functions of position or momentum operators) for many physical properties. A few latest reviews^[1–5] on trajectory-based methods for describing quantum dynamical effects are available for the semiclassical initial value representations (SC-IVRs),^[11–24] derivative forward-backward semiclassical dynamics (FBSD),^[25,26] centroid MD (CMD),^[27–29] ring polymer MD (RPMD),^[30–32] and so forth.

An important property that a practical and versatile method for studying most thermal correlation functions of complex (large) molecular systems should have is to treat both linear and *nonlinear* operators equally well and recover exact correlation functions in the classical ($\hbar \rightarrow 0$), high temperature ($\beta \rightarrow 0$), and harmonic limits.^[33–41] The linearized semiclassical initial value representation (LSC-IVR) of Miller et al.^[42–47] (or the classical Wigner model for the correlation function) is a trajectory-based method that gives exact results in the three limits even for nonlinear operators. Because the linearization approximation originally proposed in the SC-IVR^[42,43,47] can be used in the path integral representation of the correlation function to rederive the LSC-IVR/classical Wigner,^[45,48] it is sometimes termed the linearized path integral (LPI) method.^[48–51]

J. Liu

Beijing National Laboratory for Molecular Sciences, Institute of Theoretical and Computational Chemistry, College of Chemistry and Molecular Engineering, Peking University, Beijing, 100871, China
E-mail: jianliupku@pku.edu.cn

Contract grant sponsor: Recruitment Program of Global Experts

Disclosure Statement: The author is not aware of any affiliations, memberships, funding, or financial holding that might be perceived as affecting the objectivity of the article.

Contract grant sponsor: National Science Foundation of China (NSFC); contract grant number: 21373018.

© 2015 Wiley Periodicals, Inc.

Jian Liu received his PhD in Physical Chemistry in 2005 from the University of Illinois at Urbana-Champaign. He then spent a postdoc at the University of California, Berkeley and a research associate at Stanford University before he joined Peking University as an associated professor in December 2012. His research interest has focused on the development of trajectory-based quantum dynamical methods for complex (large) molecular systems.



We note that the Feynman–Kleinert approximation^[52–54] (FKA), the thermal Gaussian approximations (TGA) in the position state (also termed variational Gaussian wavepacket),^[55–57] and the TGA in the coherent state representation^[58] for treating the Boltzmann operator $e^{-\beta\hat{H}}$ in the quantum correlation function Eq. (1) have been combined with the LSC-IVR/classical Wigner to study model systems and simple liquids.^{[37,38,48,49],[59–64]} For example, Ref. [49] presents a review on using the FKA with the LSC-IVR/LPI/classical Wigner model. However, these methods request Gaussian averages of potential surfaces and forces, which become computational demanding for complex molecular systems where angle and dihedral interactions or/and induced dipole–dipole interactions are important and accurate polynomial, exponential, or Gaussian fitting of potential surfaces is often intractable.

Imaginary time path integral (via either Monte Carlo or MD) can in principle produce exact thermodynamic properties and accurate distributions of configurations. The LSC-IVR/classical Wigner combined with imaginary time path integral^[44,65] offers a more promising tool for studying general real systems, because such an approach does *not* require any specific form of the potential energy surface and are then in principle feasible to be combined with general force fields or *ab initio* calculations on the fly. Another practical way that has this property is to combine the LSC-IVR/classical Wigner with the quantum thermal bath (QTB) method^[66] as suggested in Refs. [67,68]. So the article focuses more on most recent advances under these directions. We review the underlying theory and the algorithms for implementation, while we cover most recent applications and limitations of the LSC-IVR/classical Wigner.

Theory

Below, we review derivations for the LSC-IVR/classical Wigner model for the correlation function.

Derivation of the LSC-IVR/classical Wigner model in the semiclassical framework

The Lagrangian of the system defined by Eq. (3) in classical mechanics is

$$L(\mathbf{x}, \dot{\mathbf{x}}, t) = \frac{1}{2} \dot{\mathbf{x}}^T \mathbf{M} \dot{\mathbf{x}} - V(\mathbf{x}) \quad (4)$$

and the momentum vector is

$$\mathbf{p} = \frac{\partial L}{\partial \dot{\mathbf{x}}}. \quad (5)$$

The Euler-Lagrange equation states

$$\frac{d}{dt} \frac{\partial L(\mathbf{x}, \dot{\mathbf{x}}, t)}{\partial \dot{\mathbf{x}}} - \frac{\partial L(\mathbf{x}, \dot{\mathbf{x}}, t)}{\partial \mathbf{x}} = 0 \quad (6)$$

and the action along a classical trajectory is

$$S_{\text{cl}} = \int_0^t L(\mathbf{x}, \dot{\mathbf{x}}, \tau) d\tau. \quad (7)$$

The quantity δS_{cl} is then

$$\delta S_{\text{cl}} = \int_0^t \left[\frac{\partial L}{\partial \dot{\mathbf{x}}} \delta \dot{\mathbf{x}} + \frac{\partial L}{\partial \mathbf{x}} \delta \mathbf{x} \right] d\tau. \quad (8)$$

Integration by parts for the first term of the right-hand side (RHS) of Eq. (8) leads to

$$\delta S_{\text{cl}} = \frac{\partial L}{\partial \dot{\mathbf{x}}} \delta \mathbf{x} \Big|_0^t + \int_0^t \left[- \left(\frac{d}{dt} \frac{\partial L}{\partial \dot{\mathbf{x}}} \right) \delta \mathbf{x} + \frac{\partial L}{\partial \mathbf{x}} \delta \mathbf{x} \right] d\tau = \mathbf{p}_t \delta \mathbf{x}_t - \mathbf{p}_0 \delta \mathbf{x}_0. \quad (9)$$

Then one obtains

$$\frac{\partial S_{\text{cl}}}{\partial \mathbf{x}_0} = -\mathbf{p}_0. \quad (10)$$

A stationary phase approximation to the real time path integral representation of $\langle \mathbf{x}_t | e^{-i\hat{H}t/\hbar} | \mathbf{x}_0 \rangle$ gives^[12,69]

$$\langle \mathbf{x}_t | e^{-i\hat{H}t/\hbar} | \mathbf{x}_0 \rangle \approx \sum_{\text{all classical trajectories}} \left[\det \left(\frac{i}{2\pi\hbar} \frac{\partial^2 S_{\text{cl}}}{\partial \mathbf{x}_0 \partial \mathbf{x}_t} \right) \right]^{1/2} e^{iS_{\text{cl}}/\hbar}, \quad (11)$$

where the sum is over all the classical trajectories that start from \mathbf{x}_0 and end at \mathbf{x}_t . The semiclassical approximation for the evolution operator is

$$e^{-i\hat{H}t/\hbar} \approx \int d\mathbf{x}_0 d\mathbf{x}_t \sum_{\text{all classical trajectories}} \left[\det \left(\frac{i}{2\pi\hbar} \frac{\partial^2 S_{\text{cl}}}{\partial \mathbf{x}_0 \partial \mathbf{x}_t} \right) \right]^{1/2} e^{iS_{\text{cl}}/\hbar} | \mathbf{x}_t \rangle \langle \mathbf{x}_0 |. \quad (12)$$

Note the equality

$$\sum_{\text{all classical trajectories}} \int d\mathbf{x}_t = \int d\mathbf{p}_0 \left| \frac{\partial \mathbf{x}_t}{\partial \mathbf{p}_0} \right| \quad (13)$$

holds. Applying Eqs. (10) and (13) to Eq. (12), one obtains the Van-Vleck semiclassical initial value representation (SC-IVR) for the evolution operator^[1,2,12,13]

$$e^{-i\hat{H}t/\hbar} \approx \int d\mathbf{x}_0 d\mathbf{p}_0 \left[\det \left(\frac{1}{2i\pi\hbar} \frac{\partial \mathbf{x}_t}{\partial \mathbf{p}_0} \right) \right]^{1/2} e^{iS_{cl}/\hbar} |\mathbf{x}_t\rangle \langle \mathbf{x}_0|. \quad (14)$$

Then the evolution operator backward in time is

$$e^{i\hat{H}t/\hbar} \approx \int d\mathbf{x}'_0 d\mathbf{p}'_0 \left[\det \left(\frac{1}{-2i\pi\hbar} \frac{\partial \mathbf{x}'_t}{\partial \mathbf{p}'_0} \right) \right]^{1/2} e^{-iS'_{cl}/\hbar} |\mathbf{x}'_t\rangle \langle \mathbf{x}'_0|. \quad (15)$$

The semiclassical approximation for the thermal correlation function Eq. (1) becomes

$$C_{AB}(t) \approx \frac{1}{Z} \frac{1}{(2\pi\hbar)^N} \int d\mathbf{x}_0 d\mathbf{p}_0 \int d\mathbf{x}'_0 d\mathbf{p}'_0 \left[\det \left(\frac{\partial \mathbf{x}_t}{\partial \mathbf{p}_0} \frac{\partial \mathbf{x}'_t}{\partial \mathbf{p}'_0} \right) \right]^{1/2} e^{i(S_{cl} - S'_{cl})/\hbar} \langle \mathbf{x}'_t | \hat{B} | \mathbf{x}_t \rangle \langle \mathbf{x}_0 | \hat{A} | \mathbf{x}'_0 \rangle. \quad (16)$$

Change to sum and difference variables,

$$\begin{aligned} \bar{\mathbf{x}}_0 &= \frac{\mathbf{x}_0 + \mathbf{x}'_0}{2}, \Delta \bar{\mathbf{x}}_0 = \mathbf{x}_0 - \mathbf{x}'_0 \\ \bar{\mathbf{p}}_0 &= \frac{\mathbf{p}_0 + \mathbf{p}'_0}{2}, \Delta \bar{\mathbf{p}}_0 = \mathbf{p}_0 - \mathbf{p}'_0 \end{aligned} \quad (17)$$

and expand all quantities in the integrand of Eq. (16) to first order in $\Delta \bar{\mathbf{x}}_0$ and $\Delta \bar{\mathbf{p}}_0$. Here, one makes the (rather drastic) approximation of assuming that the dominant contribution to the double phase space average comes from phase points $(\mathbf{x}_0, \mathbf{p}_0)$ and $(\mathbf{x}'_0, \mathbf{p}'_0)$ that are close to one another.^[42,43] The position at time t starting from $(\bar{\mathbf{x}}_0, \bar{\mathbf{p}}_0)$ is

$$\bar{\mathbf{x}}_t(\bar{\mathbf{x}}_0, \bar{\mathbf{p}}_0) = \frac{\mathbf{x}_t + \mathbf{x}'_t}{2}. \quad (18)$$

The difference at time t is

$$\Delta \bar{\mathbf{x}}_t \equiv \mathbf{x}_t - \mathbf{x}'_t \approx \frac{\partial \bar{\mathbf{x}}_t}{\partial \bar{\mathbf{x}}_0} \Delta \bar{\mathbf{x}}_0 + \frac{\partial \bar{\mathbf{x}}_t}{\partial \bar{\mathbf{p}}_0} \Delta \bar{\mathbf{p}}_0. \quad (19)$$

and then

$$\frac{\partial \Delta \bar{\mathbf{x}}_t}{\partial \Delta \bar{\mathbf{p}}_0} = \frac{\partial \bar{\mathbf{x}}_t}{\partial \bar{\mathbf{p}}_0}. \quad (20)$$

So one has

$$d\Delta \bar{\mathbf{x}}_0 \left[\frac{\partial \bar{\mathbf{x}}_t}{\partial \bar{\mathbf{p}}_0} \Big|_{d\Delta \bar{\mathbf{p}}_0} \right] = d\Delta \bar{\mathbf{x}}_0 d\Delta \bar{\mathbf{x}}_t. \quad (21)$$

Further, it is trivial to show

$$\frac{\partial \mathbf{x}_t}{\partial \mathbf{p}_0} = \frac{\partial \bar{\mathbf{x}}_t}{\partial \bar{\mathbf{p}}_0} + \frac{\partial^2 \bar{\mathbf{x}}_t}{\partial \bar{\mathbf{p}}_0 \partial \bar{\mathbf{x}}_0} \frac{\Delta \bar{\mathbf{x}}_0}{4} + \frac{\partial^2 \bar{\mathbf{x}}_t}{\partial \bar{\mathbf{p}}_0^2} \frac{\Delta \bar{\mathbf{p}}_0}{4} + \dots \quad (22)$$

and

$$\frac{\partial \mathbf{x}'_t}{\partial \mathbf{p}'_0} = \frac{\partial \bar{\mathbf{x}}_t}{\partial \bar{\mathbf{p}}_0} - \frac{\partial^2 \bar{\mathbf{x}}_t}{\partial \bar{\mathbf{p}}_0 \partial \bar{\mathbf{x}}_0} \frac{\Delta \bar{\mathbf{x}}_0}{4} - \frac{\partial^2 \bar{\mathbf{x}}_t}{\partial \bar{\mathbf{p}}_0^2} \frac{\Delta \bar{\mathbf{p}}_0}{4} + \dots, \quad (23)$$

then one obtains

$$\frac{\partial \mathbf{x}_t}{\partial \mathbf{p}_0} \frac{\partial \mathbf{x}'_t}{\partial \mathbf{p}'_0} \approx \left(\frac{\partial \bar{\mathbf{x}}_t}{\partial \bar{\mathbf{p}}_0} \right)^2. \quad (24)$$

Equation (9) leads to

$$S_{cl}(\mathbf{x}_0, \mathbf{p}_0) - S'_{cl}(\mathbf{x}'_0, \mathbf{p}'_0) \approx \bar{\mathbf{p}}_t \Delta \bar{\mathbf{x}}_t - \bar{\mathbf{p}}_0 \Delta \bar{\mathbf{x}}_0. \quad (25)$$

Substituting Eqs. (17), (21), (24), and (25) into Eq. (16), one obtains

$$\begin{aligned} C_{AB}(t) &\approx \frac{1}{Z} \frac{1}{(2\pi\hbar)^N} \int d\bar{\mathbf{x}}_0 d\bar{\mathbf{p}}_0 \int d\Delta \bar{\mathbf{x}}_0 d\Delta \bar{\mathbf{x}}_t \\ &\quad \times \exp [i(\Delta \bar{\mathbf{x}}_t^T \bar{\mathbf{p}}_t - \Delta \bar{\mathbf{x}}_0^T \bar{\mathbf{p}}_0) / \hbar] \\ &\quad \times \langle \bar{\mathbf{x}}_t - \frac{\Delta \bar{\mathbf{x}}_t}{2} | \hat{B} | \bar{\mathbf{x}}_t + \frac{\Delta \bar{\mathbf{x}}_t}{2} \rangle \langle \bar{\mathbf{x}}_0 + \frac{\Delta \bar{\mathbf{x}}_0}{2} | \hat{A} | \bar{\mathbf{x}}_0 - \frac{\Delta \bar{\mathbf{x}}_0}{2} \rangle. \end{aligned} \quad (26)$$

Change the variables $(\bar{\mathbf{x}}_0, \bar{\mathbf{p}}_0)$ to $(\mathbf{x}_0, \mathbf{p}_0)$. Eq. (26) then becomes

$$C_{AB}(t) \approx \frac{1}{Z} \int d\mathbf{x}_0 d\mathbf{p}_0 A_W^\beta(\mathbf{x}_0, \mathbf{p}_0) B_W(\mathbf{x}_t, \mathbf{p}_t), \quad (27)$$

which is the LSC-IVR formulation originally obtained by Miller et al.^[42,43,47] Here, $A_W^\beta(\mathbf{x}, \mathbf{p})$ is

$$A_W^\beta(\mathbf{x}, \mathbf{p}) = \frac{1}{(2\pi\hbar)^N} \int d\mathbf{y} \langle \mathbf{x} - \frac{\mathbf{y}}{2} | \hat{A}^\beta | \mathbf{x} + \frac{\mathbf{y}}{2} \rangle e^{i\mathbf{y}^T \mathbf{p} / \hbar}, \quad (28)$$

and $B_W(\mathbf{x}, \mathbf{p})$ is

$$B_W(\mathbf{x}, \mathbf{p}) = \int d\mathbf{y} \langle \mathbf{x} - \frac{\mathbf{y}}{2} | \hat{B} | \mathbf{x} + \frac{\mathbf{y}}{2} \rangle e^{i\mathbf{y}^T \mathbf{p} / \hbar}. \quad (29)$$

For convenience, one can define the function $f_{A^\beta}^W(\mathbf{x}, \mathbf{p})$ as

$$f_{A^\beta}^W(\mathbf{x}, \mathbf{p}) = \frac{A_W^\beta(\mathbf{x}, \mathbf{p})}{\rho_W^{eq}(\mathbf{x}, \mathbf{p})} = \frac{\int d\mathbf{y} \langle \mathbf{x} - \frac{\mathbf{y}}{2} | \hat{A}^\beta | \mathbf{x} + \frac{\mathbf{y}}{2} \rangle e^{i\mathbf{y}^T \mathbf{p} / \hbar}}{\int d\mathbf{y} \langle \mathbf{x} - \frac{\mathbf{y}}{2} | e^{-\beta \hat{H}} | \mathbf{x} + \frac{\mathbf{y}}{2} \rangle e^{i\mathbf{y}^T \mathbf{p} / \hbar}}. \quad (30)$$

Then the thermal correlation function Eq. (27) becomes

$$C_{AB}(t) = \frac{1}{Z} \int d\mathbf{x}_0 \int d\mathbf{p}_0 \rho_W^{eq}(\mathbf{x}_0, \mathbf{p}_0) f_{A^\beta}^W(\mathbf{x}_0, \mathbf{p}_0) B_W(\mathbf{x}_t, \mathbf{p}_t). \quad (31)$$

Eq. (27) or Eq. (31) is also termed the "classical Wigner" model for the correlation function, which has been obtained by a variety of formulations.^[46,48,65,70] The approximation postulated in Ref. [71]

$$C_{AB}(t) \approx \frac{1}{Z} \int d\mathbf{x}_0 d\mathbf{p}_0 \rho_W^{eq}(\mathbf{x}_0, \mathbf{p}_0) A_{cl}(\mathbf{x}_0) B_{cl}(\mathbf{x}_t) \quad (32)$$

[for only position dependent operators \hat{A} and \hat{B}] is *not* the same as the LSC-IVR/classical Wigner because $f_{A^\beta}^W(\mathbf{x}_0, \mathbf{p}_0)$ is often not equivalent to $A_{cl}(\mathbf{x}_0)$. Equation (32) does not recover the correct result when \hat{A} is a nonlinear operator, even in the harmonic limit. Although the classical Wigner model is an old idea,^[72-75] it is not entirely *trivial* to derive Eq. (27) or Eq. (31) for the quantum correlation function.

As extensively discussed in Refs. [1,2,44], it is informative to realize that the classical Wigner model is contained within the general SC-IVR formulation, namely, as a specific approximation to it; [42,43] more accurate implementations of the SC-IVR approach [2,23,76] would be expected to lead to a more accurate description. The LSC-IVR/classical Wigner is a short-time approximation to quantum dynamics for general systems because the approximation that the dominant contribution comes from forward and backward trajectories that are close to one another becomes more faithful as $t \rightarrow 0^+$.

It should also be noted that there are other approximate routes which lead to the classical Wigner model for correlation functions (other than simply postulating it). Shi and Geva rederived the LSC-IVR by linearizing forward and backward paths in a Feynman path integral representation of the forward and backward propagators, [45] as did Poulsen et al. somewhat later [48] using the FKA for the LSC-IVR/Classical Wigner model (they called it the FK-LPI [48,49,59–61]). As the linearization approximation is also invoked, we do not repeat the derivation but direct readers to Section III of Ref. [45] or Section II-A of Ref. [48].

Derivation of the LSC-IVR/classical Wigner model in the phase space formulation of quantum mechanics

Interestingly, although the classical Wigner model for computing dynamical properties (e.g., $\langle \hat{B}(t) \rangle$) was proposed many years ago, [72–75] to our best knowledge, it was first in Ref. [70] that the LSC-IVR/classical Wigner model for calculating general time correlation functions $\langle \hat{A}(0)\hat{B}(t) \rangle$ [for any form of \hat{A}^β and for any operator \hat{A} (or \hat{B}) in Eq. (1)] was derived in the phase space formulation of quantum mechanics. [77] Previously, derivations of the LSC-IVR/classical Wigner used approximations for the forward (backward) evolution operator $e^{-i\hat{H}t/\hbar}$ ($e^{i\hat{H}t/\hbar}$). The key step of Ref. [70] is to define a “general density operator” $\hat{A}^\beta(t) = e^{-i\hat{H}t/\hbar} \hat{A}^\beta e^{i\hat{H}t/\hbar}$, then the correlation function Eq. (1) becomes

$$C_{AB}(t) = \frac{1}{Z} \text{Tr}(\hat{A}^\beta(t)\hat{B}). \quad (33)$$

When $\hat{A} = 1$ the “general density operator” is the Boltzmann density operator $\hat{A}^\beta(t) = \hat{\rho}^{\text{eq}}(t) = e^{-i\hat{H}t/\hbar} e^{-\beta\hat{H}} e^{i\hat{H}t/\hbar}$.

The general expression of Eq. (33) in the phase space formulation of quantum mechanics [78] is

$$C_{AB}(t) = \frac{1}{Z} \int d\mathbf{x} \int d\mathbf{p} A^\beta(\mathbf{x}, \mathbf{p}; t) \tilde{B}(\mathbf{x}, \mathbf{p}). \quad (34)$$

Here, the “general” phase space distribution $A^\beta(\mathbf{x}, \mathbf{p}; t)$ and the function $\tilde{B}(\mathbf{x}, \mathbf{p})$ can be expressed in the unified classification scheme of Cohen [79] given by the following equations [78]

$$A^\beta(\mathbf{x}, \mathbf{p}; t) = \frac{1}{(2\pi)^{2N}} \int d\zeta \int d\eta \text{Tr} \left[\hat{A}^\beta(t) e^{i\zeta^T \hat{\mathbf{x}} + i\eta^T \hat{\mathbf{p}}} f(\zeta, \eta) \right] e^{-i\zeta^T \mathbf{x} - i\eta^T \mathbf{p}} \quad (35)$$

and

$$\tilde{B}(\mathbf{x}, \mathbf{p}) = \left(\frac{\hbar}{2\pi} \right)^N \int d\zeta \int d\eta \text{Tr} \left[f(-\zeta, -\eta)^{-1} e^{i\zeta^T \hat{\mathbf{x}} + i\eta^T \hat{\mathbf{p}}} \hat{B} \right] e^{-i\zeta^T \mathbf{x} - i\eta^T \mathbf{p}}. \quad (36)$$

(See Appendix A for proof.) When the function $f(\zeta, \eta) = 1$, the Wigner phase space representation is obtained, [70] that is, Eq. (34) becomes

$$C_{AB}(t) = \frac{1}{Z} \int d\mathbf{x} \int d\mathbf{p} A_W^\beta(\mathbf{x}, \mathbf{p}; t) B_W(\mathbf{x}, \mathbf{p}) \quad (37)$$

with the Wigner functions defined as

$$A_W^\beta(\mathbf{x}, \mathbf{p}; t) = \frac{1}{(2\pi\hbar)^N} \int d\mathbf{y} \left\langle \mathbf{x} - \frac{\mathbf{y}}{2} \left| \hat{A}^\beta(t) \right| \mathbf{x} + \frac{\mathbf{y}}{2} \right\rangle e^{i\mathbf{y}^T \mathbf{p}/\hbar}, \quad (38)$$

and

$$B_W(\mathbf{x}, \mathbf{p}) = \int d\mathbf{y} \left\langle \mathbf{x} - \frac{\mathbf{y}}{2} \left| \hat{B} \right| \mathbf{x} + \frac{\mathbf{y}}{2} \right\rangle e^{i\mathbf{y}^T \mathbf{p}/\hbar}. \quad (39)$$

(Also see Appendix A for proof.)

Note that the quantum Liouville equation still holds for evolution of the “general density operator”,

$$\frac{\partial \hat{A}^\beta(t)}{\partial t} = -\frac{1}{i\hbar} [\hat{A}^\beta(t), \hat{H}]. \quad (40)$$

Eq. (40) in the Wigner phase space representation becomes [70,78]

$$\frac{\partial A_W(\mathbf{x}, \mathbf{p}; t)}{\partial t} = -\left(\frac{\partial A_W}{\partial \mathbf{x}} \right)^T \mathbf{M}^{-1} \mathbf{p} + \left(\frac{\partial A_W}{\partial \mathbf{p}} \right)^T \mathbf{V}'(\mathbf{x}) - \frac{\hbar^2}{24} \frac{\partial^3 A_W}{\partial \mathbf{p}^3} V^{(3)}(\mathbf{x}) + \dots, \quad (41)$$

which is a generalization of the Wigner-Moyal equation. [72,80] [See Appendix B for proof.] It is trivial to verify that the third term and higher order terms of the RHS of Eq. (41) become zero in the classical ($\hbar \rightarrow 0$), high temperature ($\beta \rightarrow 0$), and harmonic limits. That is

$$\frac{\partial A_W(\mathbf{x}, \mathbf{p}; t)}{\partial t} = -\left(\frac{\partial A_W}{\partial \mathbf{x}} \right)^T \mathbf{M}^{-1} \mathbf{p} + \left(\frac{\partial A_W}{\partial \mathbf{p}} \right)^T \mathbf{V}'(\mathbf{x}), \quad (42)$$

which shares exactly the same form as the classical Liouville equation. So Eq. (42) leads to evaluating Eq. (37) along classical trajectories, which gives the LSC-IVR or classical Wigner model for the correlation function [Eq. (27) or Eq. (31)]. Eq. (41) suggests that the LSC-IVR produces exact thermal correlation functions in the classical, high temperature, and harmonic limits, irrespective of whether \hat{A} (or \hat{B}) is a linear or nonlinear operator. [37,38,70,78] Nevertheless, Eq. (42) is a short time approximation to the exact dynamics Eq. (41) for general systems, because the term $-\frac{\hbar^2}{24} \frac{\partial^3 A_W}{\partial \mathbf{p}^3} V^{(3)}(\mathbf{x})$ and higher order ones in Eq. (41) can make important contributions to long time dynamics.

It is straightforward to verify that the mapping Hamiltonian in the Wigner phase space [i.e., Eq. (39) when $\hat{B} = \hat{H}$] is simply the classical Hamiltonian H_{cl} . So the LSC-IVR is a kind of

trajectory-based dynamics in the phase space formulation of quantum mechanics, which conserves the mapping Hamiltonian, that is,

$$\frac{dH_W(\mathbf{x}, \mathbf{p})}{dt} = 0. \quad (43)$$

Eq. (43) is a counterpart to the quantum commutation

$$[\hat{H}, e^{-i\hat{H}t/\hbar}] = 0. \quad (44)$$

Given $\hat{A}=1$ and $\hat{B}=\hat{H}$ in the thermal correlation function Eq. (1), it becomes the average total energy at time t

$$\langle E(t) \rangle \equiv \langle \hat{H}(t) \rangle = \frac{1}{Z} \text{Tr} \left(e^{-\beta\hat{H}} e^{i\hat{H}t/\hbar} \hat{H} e^{-i\hat{H}t/\hbar} \right). \quad (45)$$

The average total energy can be decomposed into a sum of energy partitioned on each eigenstate.

$$\langle E(t) \rangle = \sum_n \langle E(t) \rangle_n, \quad (46)$$

with

$$\langle E(t) \rangle_n = \text{Tr} \left(\frac{1}{Z} e^{-\beta E_n} |n\rangle \langle n| e^{i\hat{H}t/\hbar} \hat{H} e^{-i\hat{H}t/\hbar} \right). \quad (47)$$

In quantum mechanics, both the total energy [Eq. (45)] and the energy partitioned on each eigenstate [Eq. (47)] are invariant with time. While the LSC-IVR/classical Wigner expression of Eq. (45) is

$$\langle E(t) \rangle \approx \frac{1}{Z} \int d\mathbf{x}_0 d\mathbf{p}_0 \left[e^{-\beta\hat{H}} \right]_W(\mathbf{x}_0, \mathbf{p}_0) H_W(\mathbf{x}_t, \mathbf{p}_t), \quad (48)$$

that of Eq. (47) is

$$\langle E(t) \rangle_n \approx \frac{1}{Z} \int d\mathbf{x}_0 d\mathbf{p}_0 \left[e^{-\beta E_n} |n\rangle \langle n| \right]_W(\mathbf{x}_0, \mathbf{p}_0) H_W(\mathbf{x}_t, \mathbf{p}_t). \quad (49)$$

Conservation of the mapping energy [Eq. (43)] suggests that both $\langle E(t) \rangle$ and $\langle E(t) \rangle_n$ are time-invariant in the framework. That is, the LSC-IVR/classical Wigner conserves not only the total energy but also its ‘microscopic’ term partitioned on the eigenstate. As comparison, such as CMD/RPMD are also able to preserve $\langle E(t) \rangle$ but can not satisfy detailed conservation of $\langle E(t) \rangle_n$ during dynamics. The latter, however, is important when energy transfer or transport is considered in dynamical processes.

Implementation

Calculation of $B_W(\mathbf{x}, \mathbf{p})$ for operator \hat{B} in Eq. (39) is usually straightforward; in fact, \hat{B} is often a function only of coordinates or only of momenta, in which case its Wigner function is simply the classical function itself. Calculating $A_W^\beta(\mathbf{x}, \mathbf{p})$ for operator \hat{A}^β in Eq. (38), however, involves the Boltzmann operator with the total Hamiltonian of the complete system, so that carrying out the multidimensional Fourier transform to obtain it is nontrivial.

Furthermore, it is necessary to do this to obtain the distribution of initial conditions of momenta \mathbf{p}_0 for the real time trajectories. To accomplish this task, several practical approximations^[42,48,62,65] have been introduced for the LSC-IVR/classical Wigner model. More recently, a local Gaussian approximation (LGA) has been proposed to improve on all these approximations for treating imaginary frequencies.^[44] The LGA is often combined with path integral methods, though it can also be used with other approaches for sampling the Boltzmann matrix element.^[44] When imaginary frequencies are not important, a much rougher approximation^[68] for $A_W^\beta(\mathbf{x}, \mathbf{p})$ can sometimes be introduced with the QTB method.^[66]

Local Gaussian approximation

We first briefly summarize the version of LGA^[44] developed based on the local harmonic approximation (LHA) of Shi and Geva.^[65] The LGA has been implemented for a few LSC-IVR applications^[44,81,82] for molecular systems where imaginary frequencies are not negligible.

As in the standard normal-mode analysis, mass-weighted Hessian matrix elements are given by

$$H_{kl} = \frac{1}{\sqrt{m_k m_l}} \frac{\partial^2 V}{\partial x_k \partial x_l} \quad (50)$$

where m_k represents the mass of the k th degree of freedom with $3N$, the total number of degrees of freedom. The Hamiltonian around \mathbf{x} can be expanded to second-order as

$$H(\mathbf{x} + \Delta\mathbf{x}) \approx \frac{1}{2} \mathbf{p}^T \mathbf{M}^{-1} \mathbf{p} + V(\mathbf{x}) + \left(\frac{\partial V}{\partial \mathbf{x}} \right)^T \Delta\mathbf{x} + \frac{1}{2} \Delta\mathbf{x}^T \mathbf{H} \Delta\mathbf{x}. \quad (51)$$

The eigenvalues of the mass-weighted Hessian matrix produce normal-mode frequencies $\{\omega_k\}$, that is,

$$\mathbf{T}^T \mathbf{H} \mathbf{T} = \lambda \quad (52)$$

with λ a diagonal matrix with the elements $\{(\omega_k)^2\}$ and \mathbf{T} an orthogonal matrix. If \mathbf{M} is the diagonal ‘mass matrix’ with elements $\{m_k\}$, then the mass-weighted normal mode coordinates and momenta (\mathbf{X}, \mathbf{P}) are given in terms of the Cartesian variables (\mathbf{x}, \mathbf{p}) by

$$\mathbf{X} = \mathbf{T}^T \mathbf{M}^{1/2} \mathbf{x}, \quad (53)$$

$$\mathbf{P} = \mathbf{T}^T \mathbf{M}^{-1/2} \mathbf{p}, \quad (54)$$

and

$$\Delta\mathbf{X} = \mathbf{T}^T \mathbf{M}^{1/2} \Delta\mathbf{x}. \quad (55)$$

Eq. (51) can be expressed as

$$H(\mathbf{x} + \Delta\mathbf{x}) \equiv H(\mathbf{X} + \Delta\mathbf{X}) \approx \frac{1}{2} \mathbf{P}^T \mathbf{P} + V(\mathbf{X}) + \Delta\mathbf{X}^T \mathbf{F} + \frac{1}{2} \Delta\mathbf{X}^T \lambda \Delta\mathbf{X} \quad (56)$$

with \mathbf{F} as the force in the mass-weighted normal mode coordinates

$$\mathbf{F} = \mathbf{T}^T \mathbf{M}^{-1/2} \left(\frac{\partial V}{\partial \mathbf{x}} \right). \quad (57)$$

By virtue of the fact that

$$\frac{\langle x - \frac{\Delta x}{2} | e^{-\beta \hat{H}} | x + \frac{\Delta x}{2} \rangle}{\langle x | e^{-\beta \hat{H}} | x \rangle} = \exp \left[-\frac{mQ(u)}{2\hbar^2 \beta} (\Delta x)^2 \right] \quad (58)$$

for the 1-dim harmonic case which was implemented in LHA by Shi and Geva,^[65] it is straightforward to show that the density distribution in the Wigner phase space (i.e., the Wigner function of the Boltzmann operator $e^{-\beta \hat{H}}$) is given by

$$\rho_W^{\text{eq}}(\mathbf{x}, \mathbf{p}) = \langle \mathbf{x} | e^{-\beta \hat{H}} | \mathbf{x} \rangle \prod_{k=1}^{3N} \left[\left(\frac{\beta}{2\pi Q(u_k)} \right)^{1/2} \exp \left[-\beta \frac{(P_k)^2}{2Q(u_k)} \right] \right], \quad (59)$$

where $u_k = \beta \hbar \omega_k$, P_k is the k th component of the mass-weighted normal-mode momentum \mathbf{P} [in Eq. (54)] and the quantum correction factor with the LGA ansatz proposed by Liu and Miller^[44] for both real and imaginary frequencies is given by

$$Q(u) = \begin{cases} \frac{u/2}{\tanh(u/2)} \text{ for real } u \\ = \frac{1}{Q(u_i)} = \frac{\tanh(u_i/2)}{u_i/2} \text{ for imaginary } u(u = iu_i) \end{cases}. \quad (60)$$

In terms of the phase space variables (\mathbf{x}, \mathbf{p}) , Eq. (59) thus becomes

$$\rho_W^{\text{eq,LGA}}(\mathbf{x}, \mathbf{p}) = \langle \mathbf{x} | e^{-\beta \hat{H}} | \mathbf{x} \rangle \left(\frac{\beta}{2\pi} \right)^{3N/2} |\det(\mathbf{M}_{\text{therm}}^{-1}(\mathbf{x}))|^{1/2} \exp \left[-\frac{\beta}{2} \mathbf{p}^T \mathbf{M}_{\text{therm}}^{-1} \mathbf{p} \right] \quad (61)$$

with the thermal mass matrix $\mathbf{M}_{\text{therm}}$ given by

$$\mathbf{M}_{\text{therm}}^{-1}(\mathbf{x}) = \mathbf{M}^{-1/2} \mathbf{T} \mathbf{Q}(\mathbf{u})^{-1} \mathbf{T}^T \mathbf{M}^{-1/2} \quad (62)$$

and the diagonal matrix $\mathbf{Q}(\mathbf{u}) = \{Q(u_k)\}$.

The explicit form of the LSC-IVR correlation function [Eq. (27) or Eq. (31)] with the LGA is thus given by

$$C_{AB}^{\text{LSC-IVR}}(t) = \frac{1}{Z} \int d\mathbf{x}_0 \langle \mathbf{x}_0 | e^{-\beta \hat{H}} | \mathbf{x}_0 \rangle \int d\mathbf{p}_0 \prod_{k=1}^N \left[\left(\frac{\beta}{2\pi Q(u_k)} \right)^{1/2} \exp \left[-\beta \frac{(P_{0,k})^2}{2Q(u_k)} \right] \right] \times f_{A\beta}^W(\mathbf{x}_0, \mathbf{p}_0) B_W(\mathbf{x}_t, \mathbf{p}_t) \quad (63)$$

One may summarize the specific procedure for carrying out the LSC-IVR calculation with the LGA as follows:^[44]

1. Use path integral Monte Carlo (PIMC)^[83] or path integral MD (PIMD)^[84–89] to simulate the system at equilibrium.

2. At specific intervals in the PIMC (or time steps in the PIMD), randomly select one path integral bead as the initial configuration \mathbf{x}_0 for the real time dynamics. Diagonalize the mass-weighted Hessian matrix of the potential surface to obtain the local normal mode frequencies.
3. The LGA gives the Gaussian distribution for mass-weighted normal mode momenta $\prod_{k=1}^N (\beta/2\pi Q(u_k))^{1/2} \exp \left[-\beta (P_{0,k})^2 / (2Q(u_k)) \right]$ which is used to sample initial Cartesian momenta $\mathbf{p}_0 = \mathbf{M}^{1/2} \mathbf{T} \mathbf{p}_0$ for real time trajectories.
4. Run real time classical trajectories from phase space points $(\mathbf{x}_0, \mathbf{p}_0)$ and estimate the property $f_{A\beta}^W(\mathbf{x}_0, \mathbf{p}_0) B_W(\mathbf{x}_t(\mathbf{x}_0, \mathbf{p}_0), \mathbf{p}_t(\mathbf{x}_0, \mathbf{p}_0))$ for the corresponding time correlation function. $f_{A\beta}^W(\mathbf{x}_0, \mathbf{p}_0)$ is obtained from Eq. (30) with Eqs. (58) and (60).
5. Repeat steps (2)–(4) and sum up the property $f_{A\beta}^W(\mathbf{x}_0, \mathbf{p}_0) B_W(\mathbf{x}_t(\mathbf{x}_0, \mathbf{p}_0), \mathbf{p}_t(\mathbf{x}_0, \mathbf{p}_0))$ for all real time classical trajectories until a converged result is obtained.

It is worth emphasizing that *no* approximation for the potential energy surface (PES) is made in Step 1) (the evaluation of $\langle \mathbf{x} | e^{-\beta \hat{H}} | \mathbf{x} \rangle$) and Step 4) (the real time dynamics of trajectories).

During implementation of the algorithm described above, one can accelerate the application using the following two techniques:

- a. The number of path integral beads can be decreased by a factor of 4 or more using a non-Markovian generalized Langevin equation with the colored noise proposed by Ceriotti et al.^[88–90]
- b. Dominant elements of the mass-weighted Hessian matrix of the potential surface are often block-diagonal ones. The size of each block is often the degrees of freedom of a molecule. For example, consider N_{mol} molecules and the number of degrees of freedom of each molecule is N_f (the total number of degrees of freedom is then $N = N_f * N_{\text{mol}}$), the number of the mass-weighted Hessian matrix elements is decreased from N^2 to $N_{\text{mol}} N_f^2$, and work required for diagonalization is significantly reduced from $O(N^3)$ to $O(N_{\text{mol}} N_f^3)$. So numerical efforts for the LSC-IVR with the LGA can often have a linear scaling with the number of molecules of the system. (Further simplification can be introduced though.)

If one makes a further approximation on the LGA that the momentum distribution is independent of the position, that is, one replaces the local momentum distribution in Eq. (61) by a global one,^[91] then Eq. (61) becomes

$$\frac{1}{Z} \rho_W(\mathbf{x}, \mathbf{p}) \approx \frac{\langle \mathbf{x} | e^{-\beta \hat{H}} | \mathbf{x} \rangle}{Z} \rho_{\mathbf{p}}^{\text{pl}}(\mathbf{p}), \quad (64)$$

where the averaged momentum distribution $\rho_{\mathbf{p}}^{\text{pl}}(\mathbf{p})$ can be obtained from PIMC or PIMD.^[90–92] Eq. (64) has the computational advantage that it is not always necessary to calculate the Hessian matrix of the potential energy surface. While Eq. (64) is exact for harmonic systems, it is less

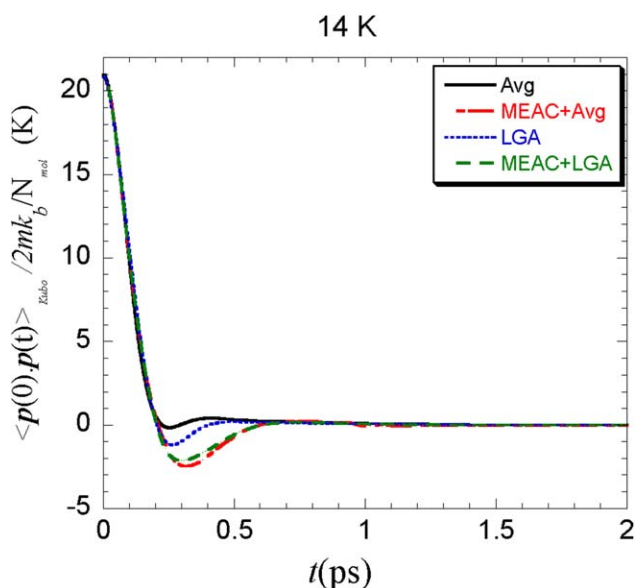


Figure 1. Kubo-transformed momentum autocorrelation functions (divided by $2mk_B N_{\text{mol}}$) based on the LSC-IVR/classical Wigner model for liquid *para*-hydrogen at the state point $T=14\text{K}$ and $v=25.6\text{cm}^3/\text{mol}$. Simulations are performed with 108 molecules in a box with the periodic boundary condition. Comparisons between the correlation functions computed from the average momentum distribution (Avg) Eq. (64) [and its MEAC-corrected version] and those obtained from the LGA Eq. (61) [and its MEAC-corrected version]. The information entropy in the MEAC procedure for the Avg result is $-1.6\text{\AA}^2/\text{ps}^2$ while that for the LGA result is only $-0.7\text{\AA}^2/\text{ps}^2$.

effective than the LGA for the LSC-IVR/classical Wigner for general molecular systems. Figure 1 compares the LSC-IVR Kubo-transformed momentum auto-correlation function for liquid *para*-hydrogen at 14 K computed from the LGA [Eq. (61)] to that obtained from the average momentum distribution [Eq. (64)]. We also use the maximum entropy analytic continuation (MEAC) to correct these LSC-IVR results (as proposed in Ref. [93]) and include them in Figure 1. The correlation function obtained from the average momentum distribution [Eq. (64)] agrees very well with that from the LGA [Eq. (61)] until 0.2 ps and then shows a shallower minimum. The MEAC-corrected correlation functions are nearly the same and are closer to the LGA result. While the information entropy in the MEAC procedure for the correlation function based on Eq. (64) is $-1.6\text{\AA}^2/\text{ps}^2$, that for the LGA result is only $-0.7\text{\AA}^2/\text{ps}^2$. (Note that the closer to zero the information entropy, the more accurate is the method. One can compare these results to those of Table I of Ref. [44]). All these suggest that the LGA [Eq. (61)] is a better approximation while the global approximation with an average momentum distribution can sometimes be useful.

Quantum thermal bath

The QTB method of Dammak et al.^[66] presents a practical approach to approximately account for quantum statistics without requesting such as Gaussian averages of potential surfaces and forces. It uses the Langevin-like equation

$$m_i \ddot{x}_{ia} = -\frac{\partial V(\mathbf{x})}{\partial x_{ia}} + R_{ia} - m_i \gamma \dot{x}_{ia} \quad (65)$$

to describe the equation of motion of the i -th atom of mass m_i . Here, x_{ia} is the a -th ($a=1, 2, \text{ or } 3$) component of the position, γ an effective frictional coefficient, and R_{ia} a Gaussian random force. The power spectral density $I_{R_{ia}R_{jb}}(\omega)$ of the Gaussian random force is related to its correlation function by the Wiener-Khinchin theorem, that is,

$$\langle R_{ia}(t)R_{jb}(t+\tau) \rangle = \frac{1}{2\pi} \int_{-\infty}^{\infty} d\omega I_{R_{ia}R_{jb}}(\omega) e^{-i\omega\tau}. \quad (66)$$

$I_{R_{ia}R_{jb}}(\omega)$ corresponds to a colored noise instead of a white one, which is related to γ by the quantum fluctuation–dissipation theorem^[94]

$$I_{R_{ia}R_{jb}}(\omega) = 2m_i \gamma \delta_{ij} \delta_{ab} \theta(\omega, T), \quad (67)$$

where

$$\theta(\omega, T) = \frac{\hbar\omega}{2\text{tanh}(\beta\hbar\omega/2)} = \frac{Q(u)}{\beta}, \quad (68)$$

δ_{ij} and δ_{ab} are the Kronecker symbol. The random force $R_{ia}(t)$ is generated from the prescribed correlation function in Eq. (66)^[66] using the numerical technique proposed by Maradudin et al.^[95] One essentially uses MD coupled to the colored noise to solve Eq. (65) to obtain the Boltzmann distribution. So the QTB method often requests less work than path integral methods and is straightforward to implement for large systems. One can verify that the correct Boltzmann distribution for a harmonic oscillator can readily be enforced in the QTB method. More importantly, the QTB method has been demonstrated as a useful approximate tool to capture quantum statistical effects for a few anharmonic systems.^[66,68]

Both the position distribution $\rho_{\mathbf{x}}(\mathbf{x})$ and the momentum distribution $\rho_{\mathbf{p}}(\mathbf{p})$ for thermal equilibrium systems can approximately be obtained by the QTB method. Basire *et al.* suggested that the Wigner function for the Boltzmann operator $e^{-\beta\hat{H}}$, that is, $\rho_W(\mathbf{x}, \mathbf{p})$ in Eq. (31), could be approximated as

$$\frac{1}{Z} \rho_W(\mathbf{x}, \mathbf{p}) \approx \rho_{\mathbf{x}}^{\text{QTB}}(\mathbf{x}) \rho_{\mathbf{p}}^{\text{QTB}}(\mathbf{p}) \quad (69)$$

in the LSC-IVR/classical Wigner model of the thermal correlation function.^[68] That is, use the position and momentum generated by the QTB method as the initial condition of the real-time classical trajectory in the LSC-IVR/classical Wigner. The work of Calvo et al. on using the QTB method for vibrational spectra^[67] can be related to the LSC-IVR/classical Wigner in a similar way. Equation (69) can be viewed as a further approximation to Eq. (64) using the QTB method rather than the path integral approach. Equation (69) with the QTB method offers a computationally efficient way to implement the LSC-IVR/classical Wigner—while the thermal statistics part uses MD with the colored noise, the real time dynamics part employs MD for the NVE ensemble.

Though not explicitly mentioned in the original literature,^[66–68] there are still two more points that we should emphasize:

1. When using the QTB method in the LSC-IVR/classical Wigner, one ought to use Eq. (31) to compute the thermal correlation function. Equation (32) is not correct for thermal correlation functions involving nonlinear operators.
2. Note that the frequency ω is *real* by definition in Eq. (66) and Eq. (67) for the QTB method. The QTB method is then expected to do little when imaginary frequencies are important for such as reaction rate problems studied in Ref. [44].

Applications

Below we briefly review illustrative applications of the LSC-IVR/classical Wigner with the two kinds of methods covered in Section 'Implementation' to a range of dynamical properties of molecular systems.

Vibrational energy relaxation in molecular liquids

The VER rate constant can be obtained by the Landau–Teller formula in terms of the Fourier transform, at the vibrational frequency, of a certain short-lived force–force correlation function. Geva and coworkers have applied the LSC-IVR to compute force–force correlation functions and then VER rates in various molecular liquids.^[65],196–99] The LHA of Shi and Geva^[65] is adequate for their applications of the LSC-IVR because imaginary frequencies are not important in the systems. The LSC-IVR results have been shown to be of the same order of magnitude as the experimental results. This demonstrates a dramatic improvement in comparison to the classical simulations of which the results are smaller than the experiment data by many orders of magnitude. For example, the LSC-IVR VER rate is $783 \pm 62 \text{ s}^{-1}$ for neat liquid O_2 at 77 K, close to the experimental result $395 \pm 18 \text{ s}^{-1}$, while the classical simulation produces $(285 \pm 31) \times 10^{-4} \text{ s}^{-1}$.^[97,99] The LSC-IVR method is able to reproduce the experimental dependence of the VER rate on temperature and that on the mole fraction.^[97] Ka and Geva have further extended the LSC-IVR applications on VER rates in real systems from diatomic molecules to polyatomic ones.^[96] Shi and Geva have also demonstrated that it is important to use a method that gives correct results for autocorrelation functions involving nonlinear operators even in the harmonic limit to study the VER rate because the force operator is nonlinear,^[33] for which the LSC-IVR/classical Wigner offers a theoretical tool while CMD does not work well.^[33]

Geva and coworkers have also shown the quantum correction factor (QCF) approach—multiplying the classical result by a frequency-dependent quantum correction factor, such as the Egelstaff or mixed harmonic-Schofield QCF,^[65],100–103] can often yield predictions of similar quality to the LSC-IVR results, but the LSC-IVR offers a more rigorous framework for studying the VER^[97] for general molecular systems.

Chemical reaction rates

Imaginary frequencies obviously play an important role in the dynamics of chemical reactions—especially tunneling effects

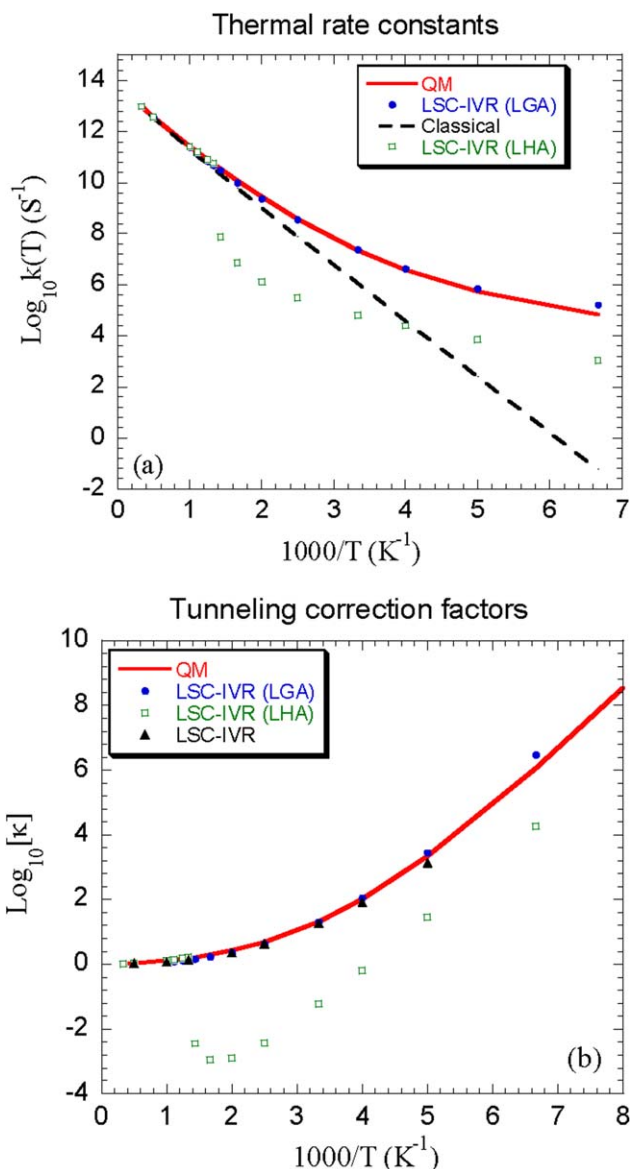


Figure 2. a) An Arrhenius plot of the thermal rate constant for the 1-d Eckart barrier. Solid line: Exact quantum results. Dotted line with solid circles: LSC-IVR results using the LGA. Dashed line: Classical results. Hollow squares: LSC-IVR results using the LHA. b) Tunneling correction factors for the 1-d Eckart barrier. Solid line: Exact quantum results. Solid circles: LSC-IVR results with the LGA. Hollow squares: LSC-IVR results with the LHA. Solid triangles: LSC-IVR results with the exact Wigner function. (Reproduced with permission from Ref. [44].)

for light atoms and low temperature—because the transition state region, the essential character of which is an imaginary frequency, is so central to the process. The LSC-IVR describes the tunneling correction for a standard 1-d Eckart model of an H atom transfer reaction quite well for temperatures down to 200K if the Wigner function is evaluated exactly, but it fails for temperatures below $\sim 700\text{K}$ if the Wigner function is evaluated by various LHAs (including the LHA of Shi and Geva^[65])—because the problem is dominated by local imaginary frequencies associated with the potential barrier. It presents a more challenging problem than the VER because the QCF approach simply fails in the imaginary frequency region.

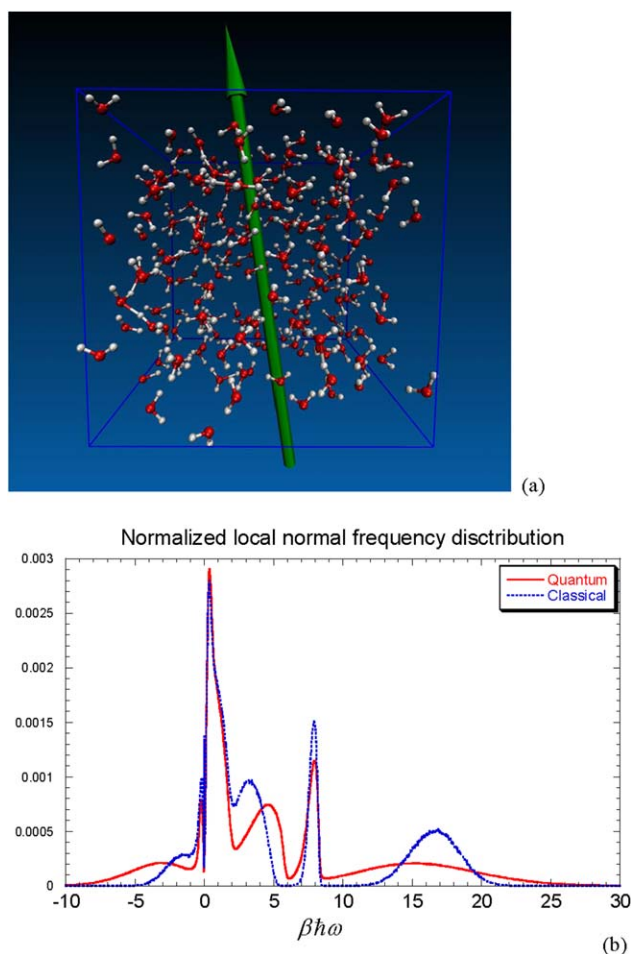


Figure 3. a) A snapshot of the collective dipole moment of liquid water (216 water molecules in a box with the periodic boundary condition). b) The normalized local normal frequency distribution of liquid water at $T=300$ K using the TTM3-F model. (Note $\hbar\beta \sim 208.5\text{cm}^{-1}$.) This is obtained from thousands of typical configurations generated from PIMD. (Fig. 3b is reproduced with permission from Ref. [81].)

The LGA^[44] described in Section ‘Local Gaussian approximation’ is able to deal with imaginary frequencies reasonably well. Figure 2 shows that the LGA gives much better results for the tunneling correction than the LHA as soon as the temperature is below the critical temperature $T_c \approx 733\text{K}$ (where the LHA results deviate from exact results by several orders of magnitude). The LGA is thus a significant improvement, giving useful results even when the tunneling correction factor is as large as 10^6 . [e.g., at $T=150\text{K}$, the exact tunneling factor is $\sim 10^6$, the classical result is off by 6 orders of magnitude, and the LSC-IVR (LGA) is correct to within a factor of 2.] The LSC-IVR (LGA) results for an analogous asymmetric Eckart barrier also demonstrate that it gives good agreement with the exact quantum results even in the deep tunneling regime.

Transport properties of liquid hydrogen and normal liquid helium

Liquid *para*-hydrogen and liquid helium are benchmark systems that have been investigated by a few approximate quantum dynamical methods. As the transport property is the zero-

frequency value of the spectrum, such as the QCF approach^[100–103] (i.e., multiplying the classical result by a frequency-dependent quantum correction factor) does not work. It has been shown imaginary local frequencies are not negligible in these low-temperature liquids.^[44] The information entropy test produced in the MEAC procedure suggests that the LSC-IVR (LGA) leads to accurate velocity correlation functions for liquid *para*-hydrogen at 25 K and 14 K.^[44] More interestingly, it has been shown the LSC-IVR works reasonably well for correlation functions even with nonlinear operators for these systems. The direct calculation of intermediate scattering functions for the dynamic structure factor using the LSC-IVR demonstrates a good agreement with the inelastic neutron scattering experiment for liquid *para*-hydrogen at 14 K.^[64] The energy current correlation function for the thermal conductivity is another example.^[104] While the classical simulations can deviate by as much as a factor of 2, less than 20% discrepancy exists between the LSC-IVR results and the experimental data for liquid *para*-hydrogen from 14 K to 32 K. Even in the normal liquid He⁴ or He³ systems where classical MD totally misses the correct physical picture, LSC-IVR is still qualitatively correct and only overestimates the thermal conductivity by a factor of ~ 2 (as shown in Ref. [104]).

IR spectrum of liquid water with the *ab initio*-based force field

Paesani et al. have first pointed out that it is not reasonable to use traditional force fields for liquid water for quantum simulations due to the double-counting problem.^[105] Although one can tune the parameters of these force fields for quantum simulations to reproduce some experimental data, a more consistent approach is to study water dynamics with *ab initio* calculations on the fly or with an *ab initio*-based flexible, polarizable force field.^{[81],[106–109]} The TTM3-F is such an *ab initio*-based model^[110] that has been used with the PIMD and several trajectory-based quantum dynamical methods for studying liquid water.^[81,107,109,111] The IR spectrum can be obtained from the collective dipole or dipole-derivative autocorrelation function, of which the dipole or dipole-derivative operator is a nonlinear one in the flexible, polarizable water model (Fig. 3a). As the time scale of the collective dipole-derivative autocorrelation function is relatively short, the LSC-IVR (LGA) then provides a theoretical tool to shed insights in understanding quantum dynamical effects in the IR spectroscopy of liquid water and to test the accuracy of the *ab initio*-based force field.^[81]

Comparison of the simulated IR spectra for the TTM3-F water model in Figure 4 shows that the intensity of the O–H stretching band given by classical MD is much higher than that by the LSC-IVR (and that of the experimental spectrum). The good agreement between the peak position of the classical O–H stretching band and experiment actually implies without ambiguity that the TTM3-F model needs to be improved for accurately describing the frequency shifts of hydrogen bonded O–H stretching vibrations, because classical MD fails to account for the significant anharmonicity of the O–H stretching vibration and yields evitable blueshifted frequencies compared to

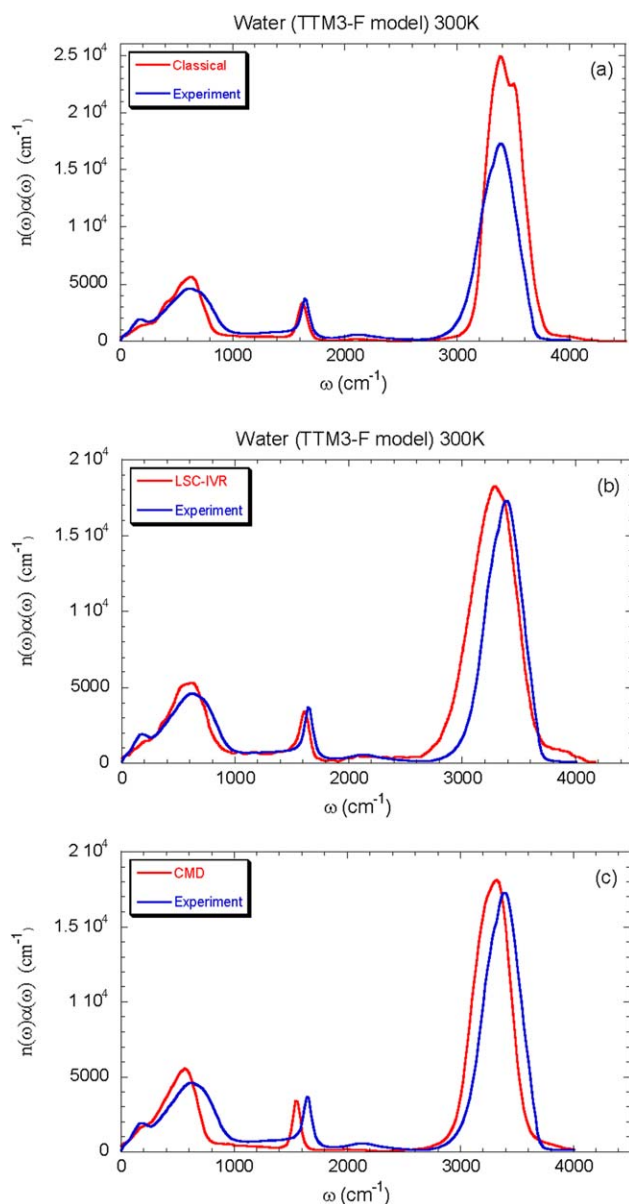


Figure 4. Comparison of simulated IR spectra using the TTM3-F model to the experimental results. (Reproduced with permission from Ref. [81].)

quantum results. The LSC-IVR librational band implies that relatively high-frequency hindered rotations ($800\text{--}1000\text{ cm}^{-1}$) still exist in liquid water for the TTM3-F model that agrees well with experiment. In agreement with experiment and similar to the discussion on the static density distribution of local frequencies (Fig. 3b), the LSC-IVR IR spectrum suggests significant quantum effects in the intermediate region ($1000\text{--}1500\text{ cm}^{-1}$) between the bending and librational bands and that ($2000\text{--}2200\text{ cm}^{-1}$) between the stretching and bending bands.^[81] The intermediate regions are believed to be sensitive to energy exchange between different modes in water.

Proton transfer spectroscopy

Basire et al. have used the LSC-IVR/classical Wigner combined with the QTB method to study a three-variable model pertinent

to proton-transfer complexes in solution (a fluctuating polar environment).^[68] The dipole correlation function and then the IR spectrum have been simulated for the weak H-bond case with the O—H frequency strongly modulated by both proton-donor-acceptor distance and the solvent and also for the solvent-induced proton transfer with the strong H-bond case where the proton is delocalized. The LSC-IVR/classical Wigner correlation functions accurately reproduce the short-time behavior of the quantum results, although disagreements appear at longer times. The spectral frequencies obtained from the LSC-IVR/classical Wigner are in good agreement with the exact results. The purely classical simulation for these model systems gives nearly identical regions for high-frequency bands but with a much too low intensity,^[68] which we expect can be greatly alleviated by using the classical dipole autocorrelation function as the Kubo-transformed one to compute the IR spectrum^[81,82,109,112] or multiplying the classical spectrum by a frequency-dependent quantum correction factor (the QCF approach).^[100–103] It will be more interesting to test the LSC-IVR/classical Wigner with the QTB method for some more challenging benchmark problems as demonstrated in the LGA applications in the previous sections.

Although the QTB method is less accurate and more limited than the imaginary time path integral approach, the LSC-IVR/classical Wigner combined with the QTB deserves attention in future as it offers an efficient approximate way for including quantum mechanical effects in MD simulations when the QTB is valid.

Limitations of the LSC-IVR/Classical Wigner

As with any approximate quantum dynamical method, the LSC-IVR/classical Wigner model of the correlation function has its limitations, which we briefly discuss below.

1. It fails to describe true quantum recurrence/rephrasing effects.^[1,2,70] Although long-time quantum recurrence/rephrasing effects (often shown in one-dimensional bounded systems) are often anticipated to be quenched by coupling among the various degrees of freedom in condensed phase systems, the LSC-IVR itself is incapable of suggesting when and where these effects do become important. The SC-IVRs^[11–24,76] offer an intrinsically consistent framework to improve over the LSC-IVR for longer time dynamics using classical trajectories.
2. It fails to conserve the mapping canonical (Boltzmann) density distribution which leads to

$$\langle \hat{B}(t) \rangle \neq \langle \hat{B}(0) \rangle \quad (70)$$

for most thermal equilibrium properties [i.e., $\hat{A}=1$ in Eq. (1)] except for harmonic systems.^[78,81,82,112–114] Because of the quantum commutation

$$\left[e^{-\beta \hat{H}}, e^{-i\hat{H}t/\hbar} \right] = 0, \quad (71)$$

it is well known that the thermal equilibrium properties are time invariant, that is,

$$\langle \hat{B}(t) \rangle \equiv \langle \hat{B}(0) \rangle. \quad (72)$$

As discussed in Ref. [82] and later in Ref. [112], the LSC-IVR/classical Wigner sometimes leads to the artificial energy flow from the intramolecular modes to the intermolecular ones. Habershon et al. termed it “the zero point energy leakage,” but this is an *inaccurate* formulation of the concept. As discussed for Eqs. (45–49) in the 2nd part of Section ‘Theory’, the LSC-IVR/classical Wigner conserves not only the total energy but also each ‘microscopic’ term, the energy partitioned on each eigenstate. Apparently, the zero point energy—the energy of the lowest eigenstate of the Hamiltonian (\hat{H}) of the system is in principle conserved in the framework of the LSC-IVR/classical Wigner as suggested by Eqs. (43) and (49). The true problem of the LSC-IVR/classical Wigner is the mapping phase distribution of the density operator is not conserved,^[78,81,82,114] that is,

$$\frac{\partial \rho(\mathbf{x}, \mathbf{p}, t)}{\partial t} \neq 0, \quad (73)$$

even though the density operator $\hat{\rho}$ commutes with the evolution operator $e^{-i\hat{H}t/\hbar}$. For instance, the energy partitioned on each eigenstate [Eq. (47)] can be divided into the kinetic energy term

$$\langle \hat{T}(t) \rangle_n = \text{Tr} \left(\frac{1}{Z} e^{-\beta E_n} |n\rangle \langle n| e^{i\hat{H}t/\hbar} \frac{1}{2} \hat{\mathbf{p}} \mathbf{M}^{-1} \hat{\mathbf{p}} e^{-i\hat{H}t/\hbar} \right) \quad (74)$$

and the potential energy term

$$\langle \hat{V}(t) \rangle_n = \text{Tr} \left(\frac{1}{Z} e^{-\beta E_n} |n\rangle \langle n| e^{i\hat{H}t/\hbar} \hat{V}(\mathbf{x}) e^{-i\hat{H}t/\hbar} \right). \quad (75)$$

While either of Eqs. (74) and (75) is constant in quantum mechanics, the LSC-IVR/classical Wigner formulation of the kinetic energy term Eq. (74) or the potential energy term Eq. (75) is not invariant with time except for harmonic systems. One can further decompose such as the potential energy term $\langle \hat{V}(t) \rangle_n$ into the intermolecular and intramolecular ones, that is, $\langle \hat{V}(t) \rangle_n = \langle \hat{V}_{\text{inter}}(t) \rangle_n + \langle \hat{V}_{\text{intra}}(t) \rangle_n$, each of which should be constant in quantum mechanics but is variant with time in the LSC-IVR/classical Wigner for general systems. That is, in the framework of the LSC-IVR/classical Wigner, the kinetic energy term and the potential energy term of the same eigenstate can exchange with each other, so do the intermolecular and intramolecular potential energy terms of the same eigenstate. In summary, while the zero point energy (and even more generally, the energy partitioned on each eigenstate) is actually preserved in the LSC-IVR/classical Wigner (therefore *no* leakage of the whole zero point energy), each component of the zero point energy is usually not time-invariant during the dynamics in this approach for equilibrium systems because of Eq. (73).^[109,112] The drawback leads to the intrinsic unphysical decay of the LSC-IVR correlation function, competition of which with the physical decay of the molecular system determines the accuracy of the LSC-IVR/classical Wigner approach.^[81]

Aiming at fixing the problem in Eq. (70) while keeping the property of the LSC-IVR/classical Wigner—giving exact correlation functions in the classical, high-temperature, harmonic limits even for nonlinear operators, one can use the theoretical framework demonstrated in the 2nd part of Section ‘Theory’ to generate the three families of trajectory-based approaches in phase space formulations of quantum mechanics^[78] that conserve the mapping canonical density distribution as discussed in Refs. [37,38,70,78]. More recently, a novel imaginary time path integral based approach—path integral Liouville dynamics (PILD)^[91] has been proposed from the framework.

Concluding Remarks

In many regards, the LSC-IVR/classical Wigner has become a versatile and mature tool that enables the inclusion of quantum mechanics effects with MD trajectories in complex molecular systems containing many interacting particles.^{[42–44,48,49],[59–61,63–65],[68,81,82,93],[96–99,104]} Its potential has been demonstrated in a great deal of applications, including reaction rates, VER rates, transport properties, spectra, and so forth, regardless of whether linear or nonlinear operators are involved. While the LSC-IVR (LGA) has already been implemented and can be accessed in several widely used molecular simulation packages such as AMBER,^[82,115] the QTB can also be readily used with the LSC-IVR.

The two kinds of methods for the LSC-IVR/classical Wigner do not require specific forms of the potential energy surface and can be straight-forward to combine with general force fields or *ab initio* electronic structure methods, which makes the LSC-IVR/classical Wigner model a useful and powerful first-principles tool for quantitatively studying various dynamical properties in complex (large) molecular systems. We hope that this article offers an effective introduction to an expanded community to use the LSC-IVR/classical Wigner in future applications in chemical, biological, or material systems.

APPENDIX A: EXPRESSION OF THE CORRELATION FUNCTION IN THE PHASE SPACE FORMULATION OF QUANTUM MECHANICS

Here, we show the proof of Eq. (34). Note that the Baker-Campbell-Hausdorff formula

$$\exp[\hat{A}] \exp[\hat{B}] = \exp \left(\hat{A} + \hat{B} + \frac{1}{2} [\hat{A}, \hat{B}] + \frac{1}{12} [\hat{A} - \hat{B}, [\hat{A}, \hat{B}]] + \dots \right) \quad (A1)$$

leads to

$$e^{i\zeta^T \hat{\mathbf{x}} + i\eta^T \hat{\mathbf{p}}} = e^{i\zeta^T \hat{\mathbf{x}}} e^{i\eta^T \hat{\mathbf{p}}} e^{i\hbar \zeta^T \eta / 2}. \quad (A2)$$

It is straightforward to show

$$e^{i\eta^T \hat{\mathbf{p}}} |\mathbf{x}\rangle = |\mathbf{x} - \hbar \eta\rangle \quad (A3)$$

by inserting the complete basis sets of the momentum operator. Implementing Eqs. (A2) and (A3) into Eq. (35) leads to

$$A^\beta(\mathbf{x}, \mathbf{p}; t) = \frac{1}{(2\pi)^{2N}} \int d\zeta \int d\boldsymbol{\eta} \int d\mathbf{y} \langle \mathbf{y} | \hat{A}^\beta(t) | \mathbf{y} - \hbar\boldsymbol{\eta} \rangle f(\zeta, \boldsymbol{\eta}) e^{i\zeta^T(\mathbf{y}-\mathbf{x})} e^{-i\boldsymbol{\eta}^T \mathbf{p}} e^{-i\hbar\zeta^T \boldsymbol{\eta}/2}. \quad (\text{A4})$$

Similarly, substituting Eqs. (A(2)) and (A(3)) into Eq. (36) and switching the variables $(\zeta, \boldsymbol{\eta})$ to $(-\zeta, -\boldsymbol{\eta})$, one obtains

$$\bar{B}(\mathbf{x}, \mathbf{p}) = \left(\frac{\hbar}{2\pi}\right)^N \int d\zeta \int d\boldsymbol{\eta} \int d\mathbf{y} f(\zeta, \boldsymbol{\eta})^{-1} \langle \mathbf{y} - \hbar\boldsymbol{\eta} | \hat{B} | \mathbf{y} \rangle e^{i\zeta^T(\mathbf{x}-\mathbf{y})} e^{i\boldsymbol{\eta}^T \mathbf{p}} e^{i\hbar\zeta^T \boldsymbol{\eta}/2}. \quad (\text{A5})$$

Using Eqs. (A(4)) and (A(5)) in the RHS of Eq. (34) and integrating it over \mathbf{x} and \mathbf{p} , the RHS of Eq. (34) becomes

$$\frac{1}{Z} \left(\frac{\hbar}{2\pi}\right)^N \int d\zeta \int d\boldsymbol{\eta} \int d\mathbf{y} \int d\zeta' \int d\boldsymbol{\eta}' \int d\mathbf{y}' \langle \mathbf{y}' | \hat{A}^\beta(t) | \mathbf{y} - \hbar\boldsymbol{\eta} \rangle f(\zeta, \boldsymbol{\eta}) e^{i\zeta^T \mathbf{y}} e^{-i\hbar\zeta^T \boldsymbol{\eta}/2} \times f(\zeta', \boldsymbol{\eta}')^{-1} \langle \mathbf{y}' - \hbar\boldsymbol{\eta}' | \hat{B} | \mathbf{y}' \rangle e^{-i\zeta'^T \mathbf{y}'} e^{i\hbar\zeta'^T \boldsymbol{\eta}'/2} \delta(\boldsymbol{\eta} - \boldsymbol{\eta}') \delta(\zeta - \zeta') \quad (\text{A6})$$

which is

$$\frac{1}{Z} \left(\frac{\hbar}{2\pi}\right)^N \int d\zeta \int d\boldsymbol{\eta} \int d\mathbf{y} \int d\mathbf{y}' \langle \mathbf{y}' | \hat{A}^\beta(t) | \mathbf{y} - \hbar\boldsymbol{\eta} \rangle e^{i\zeta^T(\mathbf{y}-\mathbf{y}')} \langle \mathbf{y}' - \hbar\boldsymbol{\eta} | \hat{B} | \mathbf{y}' \rangle. \quad (\text{A7})$$

Note that $f(\zeta, \boldsymbol{\eta})$ is now cancelled out. By integrating Eq. (A(7)) over the variable ζ and then \mathbf{y}' , it follows that

$$\frac{1}{Z} (\hbar)^N \int d\boldsymbol{\eta} \int d\mathbf{y} \langle \mathbf{y} | \hat{A}^\beta(t) | \mathbf{y} - \hbar\boldsymbol{\eta} \rangle \langle \mathbf{y} - \hbar\boldsymbol{\eta} | \hat{B} | \mathbf{y} \rangle. \quad (\text{A8})$$

Making a change of variable $\mathbf{x} = \mathbf{y} - \hbar\boldsymbol{\eta}$ in Eq. (A(8)) and integrating over both \mathbf{x} and \mathbf{y} , one obtains the LHS of Eq. (34), which proves that Eq. (34) holds for any operator \hat{A}^β or \hat{B} .

Specifically,

$$f(\zeta, \boldsymbol{\eta}) = 1 \quad (\text{A9})$$

leads to the expression of the correlation function with the Wigner^[72,116] distribution. Integrating over the variables ζ and \mathbf{y} in Eq. (A(4)) produces

$$A^\beta(\mathbf{x}, \mathbf{p}; t) = \frac{1}{(2\pi)^N} \int d\boldsymbol{\eta} \langle \mathbf{x} + \hbar\boldsymbol{\eta} | 2\hat{A}^\beta(t) | \mathbf{x} - \hbar\boldsymbol{\eta} \rangle e^{-i\boldsymbol{\eta}^T \mathbf{p}}. \quad (\text{A10})$$

By making a change of variable $\Delta\mathbf{x} = -\hbar\boldsymbol{\eta}/2$, it follows

$$A^\beta(\mathbf{x}, \mathbf{p}; t) = \frac{1}{(2\pi\hbar)^N} \int d\Delta\mathbf{x} \langle \mathbf{x} - \Delta\mathbf{x} | 2\hat{A}^\beta(t) | \mathbf{x} + \Delta\mathbf{x} \rangle e^{i\Delta\mathbf{x}^T \mathbf{p}/\hbar} \equiv A_W^\beta(\mathbf{x}, \mathbf{p}; t). \quad (\text{A11})$$

Similarly, after integrating over the variables ζ and \mathbf{y} in Eq. (A(5)) and then making a change of variable $\Delta\mathbf{x} = \hbar\boldsymbol{\eta}/2$, Eq. (A(5)) becomes

$$\bar{B}(\mathbf{x}, \mathbf{p}) = \int d\Delta\mathbf{x} \langle \mathbf{x} - \Delta\mathbf{x} | 2\hat{B} | \mathbf{x} + \Delta\mathbf{x} \rangle e^{i\Delta\mathbf{x}^T \mathbf{p}/\hbar} \equiv B_W(\mathbf{x}, \mathbf{p}). \quad (\text{A12})$$

Now Eq. (34) leads to Eq. (37).

APPENDIX B: QUANTUM LIOUVILLE EQUATION IN THE WIGNER PHASE SPACE REPRESENTATION

Here, we follow Ref. [78] to express the quantum Liouville equation (or the von Neumann equation) for the general density operator $\hat{A}^\beta(t) = e^{-i\hat{H}t/\hbar} \hat{A}^\beta e^{i\hat{H}t/\hbar}$ [i.e., Eq. (40)] in the Wigner phase space.

For any operator \hat{A} , it is trivial to show that

$$\langle \mathbf{x} - \Delta\mathbf{x} | 2\hat{p}\hat{A} | \mathbf{y} \rangle = -i\hbar \frac{\partial}{\partial \mathbf{x}} \langle \mathbf{x} - \Delta\mathbf{x} | 2\hat{A} | \mathbf{y} \rangle = 2i\hbar \frac{\partial}{\partial \Delta\mathbf{x}} \langle \mathbf{x} - \Delta\mathbf{x} | 2\hat{A} | \mathbf{y} \rangle \quad (\text{B1})$$

and

$$\langle \mathbf{y} | \hat{A}\hat{p} | \mathbf{x} + \Delta\mathbf{x} \rangle = i\hbar \frac{\partial}{\partial \mathbf{x}} \langle \mathbf{y} | \hat{A} | \mathbf{x} + \Delta\mathbf{x} \rangle = 2i\hbar \frac{\partial}{\partial \Delta\mathbf{x}} \langle \mathbf{y} | \hat{A} | \mathbf{x} + \Delta\mathbf{x} \rangle. \quad (\text{B2})$$

Based on Eqs. (B(1)) and (B(2)), one can show

$$\langle \mathbf{x} - \Delta\mathbf{x} | 2\hat{p}\hat{A} + \hat{A}\hat{p} | \mathbf{x} + \Delta\mathbf{x} \rangle = 2i\hbar \frac{\partial}{\partial \Delta\mathbf{x}} \langle \mathbf{x} - \Delta\mathbf{x} | 2\hat{A} | \mathbf{x} + \Delta\mathbf{x} \rangle \quad (\text{B3})$$

and

$$\langle \mathbf{x} - \Delta\mathbf{x} | 2\hat{A}\hat{p} - \hat{p}\hat{A} | \mathbf{x} + \Delta\mathbf{x} \rangle = i\hbar \frac{\partial}{\partial \mathbf{x}} \langle \mathbf{x} - \Delta\mathbf{x} | 2\hat{A} | \mathbf{x} + \Delta\mathbf{x} \rangle. \quad (\text{B4})$$

Note

$$\left[\hat{A}^\beta, \frac{1}{2}\hat{p}^T \mathbf{M}^{-1} \hat{p} \right] = \frac{1}{2}\hat{p}^T \mathbf{M}^{-1} \left[\hat{A}^\beta, \hat{p} \right] + \left[\hat{A}^\beta, \hat{p} \right]^T \frac{1}{2} \mathbf{M}^{-1} \hat{p}. \quad (\text{B5})$$

One can derive the following equation from Eqs. (B3)–(B5),

$$\left\langle \mathbf{x} - \frac{\Delta\mathbf{x}}{2} \left| -\frac{1}{i\hbar} \left[\hat{A}^\beta, \frac{1}{2}\hat{p}^T \mathbf{M}^{-1} \hat{p} \right] \right| \mathbf{x} + \frac{\Delta\mathbf{x}}{2} \right\rangle = -i\hbar \left(\frac{\partial}{\partial \Delta\mathbf{x}} \right)^T \mathbf{M}^{-1} \frac{\partial}{\partial \mathbf{x}} \left\langle \mathbf{x} - \frac{\Delta\mathbf{x}}{2} | \hat{A}^\beta | \mathbf{x} + \frac{\Delta\mathbf{x}}{2} \right\rangle. \quad (\text{B6})$$

Integrating by parts over $\Delta\mathbf{x}$ for the above equation leads to

$$\left(\frac{1}{2\pi\hbar} \right)^N \int_{-\infty}^{\infty} d\Delta\mathbf{x} \left[\left\langle \mathbf{x} - \frac{\Delta\mathbf{x}}{2} \left| -\frac{1}{i\hbar} \left[\hat{A}^\beta, \frac{1}{2}\hat{p}^T \mathbf{M}^{-1} \hat{p} \right] \right| \mathbf{x} + \frac{\Delta\mathbf{x}}{2} \right\rangle e^{i\mathbf{p}^T \Delta\mathbf{x}/\hbar} \right] = -\hat{p}^T \mathbf{M}^{-1} \frac{\partial}{\partial \mathbf{x}} A_W^\beta(\mathbf{x}, \mathbf{p}). \quad (\text{B7})$$

Expanding the potential $V(\mathbf{x})$ into a Taylor series, one can show

$$\left\langle \mathbf{x} - \frac{\Delta\mathbf{x}}{2} \left| \left[\hat{A}^\beta, \hat{V}(\hat{\mathbf{x}}) \right] \right| \mathbf{x} + \frac{\Delta\mathbf{x}}{2} \right\rangle = \left\langle \mathbf{x} - \frac{\Delta\mathbf{x}}{2} | \hat{A}^\beta | \mathbf{x} + \frac{\Delta\mathbf{x}}{2} \right\rangle \left[V\left(\mathbf{x} + \frac{\Delta\mathbf{x}}{2}\right) - V\left(\mathbf{x} - \frac{\Delta\mathbf{x}}{2}\right) \right] = \left\langle \mathbf{x} - \frac{\Delta\mathbf{x}}{2} | \hat{A}^\beta | \mathbf{x} + \frac{\Delta\mathbf{x}}{2} \right\rangle \left[V'(\mathbf{x})\Delta\mathbf{x} + \frac{2}{3!} V^{(3)}(\mathbf{x}) \left(\frac{\Delta\mathbf{x}}{2}\right)^3 + \dots \right]. \quad (\text{B8})$$

Here

$$V^{(3)}(\mathbf{x}) \left(\frac{\Delta\mathbf{x}}{2}\right)^3 = \frac{1}{8} \sum_{i,j,k=1}^N \frac{\partial^3 V}{\partial x_i \partial x_j \partial x_k} \Delta x_i \Delta x_j \Delta x_k. \quad (\text{B9})$$

Integrating by parts over $\Delta\mathbf{x}$ in the RHS of Eq. (B(8)), one has

$$\begin{aligned} & \left(\frac{1}{2\pi\hbar}\right)^N \int_{-\infty}^{\infty} d\Delta\mathbf{x} \left[\left\langle \mathbf{x} - \frac{\Delta\mathbf{x}}{2} \left| -\frac{1}{i\hbar} [\hat{A}^\beta, \hat{V}(\hat{\mathbf{x}})] \right| \mathbf{x} + \frac{\Delta\mathbf{x}}{2} \right\rangle e^{i\mathbf{p}^T \Delta\mathbf{x}/\hbar} \right] \\ & = \frac{\partial A_W^\beta}{\partial \mathbf{p}} V'(\mathbf{x}) - \frac{\hbar^2}{24} \frac{\partial^3 A_W^\beta}{\partial \mathbf{p}^3} V^{(3)}(\mathbf{x}) + \dots \end{aligned} \quad (\text{B10})$$

Here

$$\frac{\partial^3 A_W^\beta}{\partial \mathbf{p}^3} V^{(3)}(\mathbf{x}) = \sum_{i,j,k=1}^N \frac{\partial^3 A_W^\beta}{\partial p_i \partial p_j \partial p_k} \frac{\partial^3 V}{\partial x_i \partial x_j \partial x_k}. \quad (\text{B11})$$

Finally, Eqs. (B(7)) and (B(8)) demonstrate that the Wigner phase space representation of the Liouville equation [Eq. (40)] can be expressed as Eq. (41). Note that Eq. (41) is a generalization of the Wigner-Moyal equation^[72,80] for the conventional density operator $\hat{\rho}$. Note that \hat{A}^β in Eqs. (B(5))–(B(8)) can be replaced by any general density operator such as $\hat{\rho}\hat{A}$, for which Eq. (41) still holds.

Acknowledgments

J.L. is extremely grateful to William Miller for his support and insights throughout the collaboration on the work described in this review. We are indebted to Berni Alder, Francesco Paesani, Wei Zhang, David Case, George Fanourgakis, Sotiris Xantheas, Sho Imoto, and Shinji Saito for their valuable contributions to the LSC-IVR applications. We also acknowledge a generous allocation of supercomputing time from the National Energy Research Scientific Computing Center (NERSC) and the use of the computational cluster resources provided by the Beijing supercomputer center and by the Tianjing supercomputer center.

Keywords: quantum dynamics · phase space · correlation function · path integral · semiclassical initial value representation

How to cite this article: J., Liu *Int. J. Quantum Chem.* **2015**, *115*, 657–670. DOI: 10.1002/qua.24872

[1] W. H. Miller, *Proc. Natl. Acad. Sci. USA* **2005**, *102*, 6660.

[2] W. H. Miller, *J. Chem. Phys.* **2006**, *125*, 132305.

[3] G. A. Voth, *Adv. Chem. Phys.* **1996**, *XCIII*, 135.

[4] S. Habershon, D. E. T. E. Manolopoulos, T. Markland, F. Miller, III, *Annu. Rev. Phys. Chem.* **2013**, *64*, 387.

[5] N. Makri, A. Nakayama, N. Wright, *J. Theor. Comput. Chem.* **2004**, *3*, 391.

[6] B. J. Berne, G. D. Harp, *Adv. Chem. Phys.* **1970**, *17*, 63.

[7] R. Zwanzig, *Nonequilibrium Statistical Mechanics*; Oxford University Press: New York, **2001**.

[8] D. A. McQuarrie, *Statistical Mechanics*; University Science Books: Sausalito, CA, **2000**.

[9] W. H. Miller, S. D. Schwartz, J. W. Tromp, *J. Chem. Phys.* **1983**, *79*, 4889.

[10] R. Kubo, M. Toda, N. Hashitsume, *Statistical Physics II: Nonequilibrium Statistical Mechanics*; Springer-Verlag: Heidelberg, **1991**.

[11] W. H. Miller, *J. Chem. Phys.* **1970**, *53*, 1949.

[12] W. H. Miller, *Adv. Chem. Phys.* **1974**, *25*, 69.

[13] W. H. Miller, *Adv. Chem. Phys.* **1975**, *30*, 77.

[14] E. J. Heller, *J. Chem. Phys.* **1981**, *75*, 2923.

[15] M. F. Herman, E. Kluk, *Chem. Phys.* **1984**, *91*, 27.

[16] E. J. Heller, *J. Chem. Phys.* **1991**, *94*, 2723.

[17] W. H. Miller, *J. Chem. Phys.* **1991**, *95*, 9428.

[18] E. J. Heller, *J. Chem. Phys.* **1991**, *95*, 9431.

[19] G. Campolieti, P. Brumer, *J. Chem. Phys.* **1992**, *96*, 5969.

[20] K. G. Kay, *J. Chem. Phys.* **1994**, *100*, 4377.

[21] K. G. Kay, *Chem. Phys.* **2006**, *322*, 3.

[22] D. J. Tannor, S. Garashchuk, *Annu. Rev. Phys. Chem.* **2000**, *51*, 553.

[23] M. Thoss, H. Wang, W. H. Miller, *J. Chem. Phys.* **2001**, *114*, 9220.

[24] W. H. Miller, *J. Phys. Chem. A* **2001**, *105*, 2942.

[25] J. Shao, N. Makri, *J. Phys. Chem. A* **1999**, *103*, 7753.

[26] J. Shao, N. Makri, *J. Phys. Chem. A* **1999**, *103*, 9479.

[27] J. Cao, G. A. Voth, *J. Chem. Phys.* **1994**, *101*, 6168.

[28] J. Cao, G. A. Voth, *J. Chem. Phys.* **1994**, *100*, 5106.

[29] S. Jang, G. A. Voth, *J. Chem. Phys.* **1999**, *111*, 2371.

[30] I. R. Craig, D. E. Manolopoulos, *J. Chem. Phys.* **2004**, *121*, 3368.

[31] J. O. Richardson, S. C. Althorpe, *J. Chem. Phys.* **2009**, *131*, 214106.

[32] M. Rossi, M. Ceriotti, D. E. Manolopoulos, *J. Chem. Phys.* **2014**, *140*, 234116.

[33] Q. Shi, E. Geva, *J. Chem. Phys.* **2003**, *119*, 9030.

[34] D. R. Reichman, P. N. Roy, S. Jang, G. A. Voth, *J. Chem. Phys.* **2000**, *113*, 919.

[35] T. D. Hone, G. A. Voth, *J. Chem. Phys.* **2004**, *121*, 6412.

[36] A. Horikoshi, K. Kinugawa, *J. Chem. Phys.* **2005**, *122*, 174104.

[37] J. Liu, W. H. Miller, *J. Chem. Phys.* **2011**, *134*, 104102.

[38] J. Liu, *J. Chem. Phys.* **2011**, *134*, 194110.

[39] F. Paesani, G. A. Voth, *J. Chem. Phys.* **2008**, *129*, 194113.

[40] S. Habershon, B. J. Braams, D. E. Manolopoulos, *J. Chem. Phys.* **2007**, *127*, 174108.

[41] I. R. Craig, D. E. Manolopoulos, *Chem. Phys.* **2006**, *322*, 236.

[42] H. Wang, X. Sun, W. H. Miller, *J. Chem. Phys.* **1998**, *108*, 9726.

[43] X. Sun, H. Wang, W. H. Miller, *J. Chem. Phys.* **1998**, *109*, 7064.

[44] J. Liu, W. H. Miller, *J. Chem. Phys.* **2009**, *131*, 074113.

[45] Q. Shi, E. Geva, *J. Chem. Phys.* **2003**, *118*, 8173.

[46] E. Pollak, J. L. Liao, *J. Chem. Phys.* **1998**, *108*, 2733.

[47] R. Hernandez, G. A. Voth, *Chem. Phys.* **1998**, *233*, 243.

[48] J. A. Poulsen, G. Nyman, P. J. Rossky, *J. Chem. Phys.* **2003**, *119*, 12179.

[49] J. A. Poulsen, G. Nyman, P. J. Rossky, *J. Chem. Theory Comput.* **2006**, *2*, 1482.

[50] S. Bonella, D. Montemayor, D. F. Coker, *Proc. Natl. Acad. Sci. USA* **2005**, *102*, 6715.

[51] M. S. Causo, G. Ciccotti, D. Montemayor, S. Bonella, D. F. Coker, *J. Phys. Chem. B* **2005**, *109*, 6855.

[52] R. Giachetti, V. Tognetti, *Phys. Rev. Lett.* **1985**, *55*, 912.

[53] R. P. Feynman, H. Kleinert, *Phys. Rev. A* **1986**, *34*, 5080.

[54] A. Cuccoli, R. Giachetti, V. Tognetti, R. Vaia, P. Verrucchi, *J. Phys. Condens. Matt.* **1995**, *7*, 7891.

[55] B. Hellsing, S. I. Sawada, H. Metiu, *Chem. Phys. Lett.* **1985**, *122*, 303.

[56] P. Frantsuzov, A. Neumaier, V. A. Mandelshtam, *Chem. Phys. Lett.* **2003**, *381*, 117.

[57] J. Shao, E. Pollak, *J. Chem. Phys.* **2006**, *125*, 133502.

[58] D. H. Zhang, J. Shao, E. Pollak, *J. Chem. Phys.* **2009**, *131*, 044116.

[59] J. A. Poulsen, G. Nyman, P. J. Rossky, *J. Phys. Chem. A* **2004**, *108*, 8743.

[60] J. A. Poulsen, G. Nyman, P. J. Rossky, *Proc. Natl. Acad. Sci. USA* **2005**, *102*, 6709.

[61] J. A. Poulsen, J. Scheers, G. Nyman, P. J. Rossky, *Phys. Rev. B* **2007**, *75*, 224505.

[62] J. Liu, W. H. Miller, *J. Chem. Phys.* **2006**, *125*, 224104.

[63] J. Liu, W. H. Miller, *J. Chem. Phys.* **2007**, *127*, 114506.

[64] J. Liu, W. H. Miller, *J. Chem. Phys.* **2008**, *128*, 144511.

[65] Q. Shi, E. Geva, *J. Phys. Chem. A* **2003**, *107*, 9059.

[66] H. Dammak, Y. Chalopin, M. Laroche, M. Hayoun, J.-J. Greffet, *Phys. Rev. Lett.* **2009**, *103*, 190601.

- [67] F. Calvo, N. T. Van-Oanh, P. Parneix, C. Falvo, *Phys. Chem. Chem. Phys.* **2012**, *14*, 10503.
- [68] M. Basire, D. Borgis, R. Vuilleumier, *Phys. Chem. Chem. Phys.* **2013**, *15*, 12591.
- [69] L. S. Schulman, *Techniques and Applications of Path Integration*; Wiley: New York, **1981**.
- [70] J. Liu, W. H. Miller, *J. Chem. Phys.* **2007**, *126*, 234110.
- [71] J. Cao, G. A. Voth, *J. Chem. Phys.* **1996**, *104*, 273.
- [72] E. Wigner, *Phys. Rev.* **1932**, *40*, 749.
- [73] E. Wigner, *Trans. Faraday Soc.* **1938**, *34*, 0029.
- [74] E. J. Heller, *J. Chem. Phys.* **1976**, *65*, 1289.
- [75] H. W. Lee, M. O. Scully, *J. Chem. Phys.* **1980**, *73*, 2238.
- [76] G. H. Tao, W. H. Miller, *J. Chem. Phys.* **2011**, *135*, 024104.
- [77] H. W. Lee, *Phys. Rep.* **1995**, *259*, 147.
- [78] J. Liu, W. H. Miller, *J. Chem. Phys.* **2011**, *134*, 104101.
- [79] L. Cohen, *J. Math. Phys.* **1966**, *7*, 781.
- [80] J. E. Moyal, *Proc. Cambridge Philos. Soc.* **1949**, *45*, 99.
- [81] J. Liu, W. H. Miller, G. S. Fanourgakis, S. S. Xantheas, S. Imoto, S. Saito, *J. Chem. Phys.* **2011**, *135*, 244503.
- [82] J. Liu, W. H. Miller, F. Paesani, W. Zhang, D. A. Case, *J. Chem. Phys.* **2009**, *131*, 164509.
- [83] D. M. Ceperley, *Rev. Mod. Phys.* **1995**, *67*, 279.
- [84] D. Chandler, P. G. Wolynes, *J. Chem. Phys.* **1981**, *74*, 4078.
- [85] B. J. Berne, D. Thirumalai, *Annu. Rev. Phys. Chem.* **1986**, *37*, 401.
- [86] M. E. Tuckerman, In *Quantum Simulations of Complex Many-Body Systems: From Theory to Algorithms*; J. Grotendorst, D. Marx, A. Muramatsu, Eds.; John von Neumann Institute for Computing: Jülich, **2002**, pp. 269–298.
- [87] M. E. Tuckerman, B. J. Berne, G. J. Martyna, M. L. Klein, *J. Chem. Phys.* **1993**, *99*, 2796.
- [88] M. Ceriotti, D. E. Manolopoulos, M. Parrinello, *J. Chem. Phys.* **2011**, *134*, 084104.
- [89] M. Ceriotti, M. Parrinello, T. E. Markland, D. E. Manolopoulos, *J. Chem. Phys.* **2010**, *133*, 124104.
- [90] M. Ceriotti, D. E. Manolopoulos, *Phys. Rev. Lett.* **2012**, *109*, 100604.
- [91] J. Liu, *J. Chem. Phys.* **2014**, *140*, 224107.
- [92] L. Lin, J. A. Morrone, R. Car, M. Parrinello, *Phys. Rev. B* **2011**, *83*, 220302.
- [93] J. Liu, W. H. Miller, *J. Chem. Phys.* **2008**, *129*, 124111.
- [94] H. B. Callen, T. A. Welton, *Phys. Rev.* **1951**, *83*, 34.
- [95] A. A. Maradudin, T. Michel, A. R. McGurn, E. R. Mendez, *Ann. Phys.* **1990**, *203*, 255.
- [96] B. J. Ka, E. Geva, *J. Phys. Chem. A* **2006**, *110*, 9555.
- [97] B. J. Ka, Q. Shi, E. Geva, *J. Phys. Chem. A* **2005**, *109*, 5527.
- [98] I. Navrotskaya, E. Geva, *J. Phys. Chem. A* **2007**, *111*, 460.
- [99] Q. Shi, E. Geva, *J. Phys. Chem. A* **2003**, *107*, 9070.
- [100] P. Schofield, *Phys. Rev. Lett.* **1960**, *4*, 239.
- [101] P. A. Egelstaff, *Adv. Phys.* **1962**, *11*, 203.
- [102] S. A. Egorov, B. J. Berne, *J. Chem. Phys.* **1997**, *107*, 6050.
- [103] S. A. Egorov, K. F. Everitt, J. L. Skinner, *J. Phys. Chem.* **1999**, *103*, 9494.
- [104] J. Liu, B. J. Alder, W. H. Miller, *J. Chem. Phys.* **2011**, *135*, 114105.
- [105] F. Paesani, W. Zhang, D. A. Case, T. E. Cheatham, III, G. A. Voth, *J. Chem. Phys.* **2006**, *125*, 184507.
- [106] F. Paesani, S. Iuchi, G. A. Voth, *J. Chem. Phys.* **2007**, *127*, 074506.
- [107] F. Paesani, G. A. Voth, *J. Phys. Chem. B* **2009**, *113*, 5702.
- [108] F. Paesani, S. S. Xantheas, G. A. Voth, *J. Phys. Chem. B* **2009**, *113*, 13118.
- [109] S. Habershon, G. S. Fanourgakis, D. E. Manolopoulos, *J. Chem. Phys.* **2008**, *129*, 074501.
- [110] G. S. Fanourgakis, S. S. Xantheas, *J. Chem. Phys.* **2008**, *128*, 074506.
- [111] F. Paesani, S. Yoo, H. J. Bakker, S. S. Xantheas, *J. Phys. Chem. Lett.* **2010**, *1*, 2316.
- [112] S. Habershon, D. E. Manolopoulos, *J. Chem. Phys.* **2009**, *131*, 244518.
- [113] G. A. Voth, T. D. Hone, *J. Chem. Phys.* **2005**, *122*, 057102.
- [114] J. Liu, A. Nakayama, N. Makri, *Mol. Phys.* **2006**, *104*, 1267.
- [115] D. A. Case, T. E. Cheatham, T. Darden, H. Gohlke, R. Luo, K. M. Merz, A. Onufriev, C. Simmerling, B. Wang, R. J. Woods, *J. Comput. Chem.* **2005**, *26*, 1668.
- [116] E. P. Wigner, *Perspectives in Quantum Theory*; MIT: Cambridge, **1971**.

Received: 9 October 2014
Revised: 11 January 2015
Accepted: 12 January 2015
Published online 11 February 2015